2011

3D FUNCTIONAL MODELING OF DBS EFFICACY AND DEVELOPMENT OF ANALYTICAL TOOLS TO EXPLORE FUNCTIONAL STN

Deepak Kumbhare
Virginia Commonwealth University

i

3D FUNCTIONAL MODELING OF DBS EFFICACY AND DEVELOPMENT OF

ANALYTICAL TOOLS TO EXPLORE FUNCTIONAL STN

A thesis submitted in partial fulfillment of the requirements for the degree of Master of Science

at Virginia Commonwealth University.

by

DEEPAK KUMBHARE

Bachelor of Engineering, Rajiv Gandhi Technical University, Bhopal, India, 2007

Director: OU BAI, PH.D.

Assistant Professor, Department of Biomedical Engineering

Virginia Commonwealth University

Richmond, Virginia

May, 2011

Acknowledgments

I would like to express my gratitude to my adviser, Dr. Ou Bai for his continuous support throughout in my study and research. His guidance and encouragement have helped me pursuing this exciting line of research. Throughout the entire project he has encouraged me to develop independent thinking and research skills. I am extremely thankful to Dr. Kathryn Holloway for giving me the opportunity to work on this research and providing the clinical data for analysis. Her in-depth knowledge and logical way of thinking has been of great help to me. Her extensive discussions around my work and constructive comments have been very helpful throughout this project. I would like to thank Dr. V. Ramakrishnan, whose help, suggestions, patience and encouragement has helped me at all times during this research project.

I would also like to thank all my committee members, Dr. Ou Bai, Dr. Kathryn Holloway and Dr. Din-Yu Fei for all the guidance and support throughout this project. Their detailed review, constructive criticism and excellent advice have helped me immensely in completion of my thesis project and improving my skills for technical writing.

I would also like to thank my lab mates Dandan Huang, Kai Qian, Vaishnavi Karnad and Mason Montgomery for your help and support in my study.

Also, I would like to thank my friends who have been a constant source of encouragement throughout my graduate study. Last and most importantly, I would like to thank my parents for their enduring love and support throughout my life in achieving my dreams.

Contents

List of Abbreviations

PD	-	Parkinson's Disease
DBS	-	Deep Brain Stimulation
UPDRS	-	Unified Parkinson's Disease Rating Scale
STN	-	Subthalamic Nucleus
GPi	-	Globus Pallidus
AC	-	Anterior Commissure
PC	-	Posterior Commissure
ME	-	Microelectrode
MER	-	Microelectrode Recording
MSI	-	MacroStim Interface
CT	-	Computed Tomography
MRI	-	Magnetic Resonance Imaging
MIDW	-	Monopolar Inverse Weighted Distance
IDW	-	Inverse Distance Weighted Method
RWI	-	Roving Window Interpolation
BSI	-	Bipolar Simulation Interpolation
ROI	-	Region of Interest
RMSE	-	Root Mean Square Error
CV	-	Cross Validation
GUI	-	Graphic User Interface

List of Tables

List of Figures

x

ABSTRACT:

Introduction: Exploring the brain for optimal locations for deep brain stimulation (DBS) therapy is a challenging task, which can be facilitated by analysis of DBS efficacy in a large number of patients with Parkinson's disease (PD). The Unified Parkinson's Disease Rating Scale (UPDRS) scores indicate the DBS efficacy of the corresponding stimulation location in a particular patient. The spatial distribution of these clinical scores can be used to construct a functional model which closely models the expected efficacy of stimulation in the region.

Designs and Methods: In this study, different interpolation techniques were investigated that can appropriately model the DBS efficacy for Parkinson's disease patients. These techniques are linear triangulation based interpolation, 'roving window' interpolation and 'Monopolar inverse weighted distance' (MIDW) interpolation. The MIDW interpolation technique is developed on the basis of electric field geometry of the monopolar DBS stimulation electrodes, based on the DBS model of monopolar cathodic stimulation of brain tissues. Each of these models was evaluated for their predictability, interpolation accuracy, as well as other benefits and limitations. The bootstrapping based optimization method was proposed to minimize the observational and patient variability in the collected database. A simulation study was performed to validate that the statistically optimized interpolated models were capable to produce reliable efficacy contour plots and reduced false effect due to outliers. Some additional visualization and analysis tools including a graphic user interface (GUI) were also developed for better understanding of the scenario.

Results: The interpolation performance of the MIDW interpolation, the linear triangulation method and Roving window method was evaluated as interpolation error as 0.0903, 0.1219 and

0.3006 respectively. Degree of prediction for the above methods was found to be 0.0822, 0.2986 and 0.0367 respectively. The simulation study demonstrate that the mean improvement in outlier handling and increased reliability after bootstrapping based optimization (performed on Linear triangulation interpolation method) is 6.192% and 12.8775% respectively. The different interpolation techniques used to model monopolar and bipolar stimulation data is found to be useful to study the corresponding efficacy distribution. A user friendly GUI (PDRP_GUI) and other utility tools are developed.

Conclusion: Our investigation demonstrated that the MIDW and linear triangulation methods provided better degree of prediction, whereas the MIDW interpolation with appropriate configuration provided better interpolation accuracy. The simulation study suggests that the bootstrapping-based optimization can be used as an efficient tool to reduce outlier effects and increase interpolated reliability of the functional model of DBS efficacy. Additionally, the differential interpolation techniques used for monopolar and bipolar stimulation modeling facilitate study of overall DBS efficacy using the entire dataset.

CHAPTER 1 : Introduction and Background

1.1 Parkinson's Diseases

Parkinson's disease (PD) [1] [2, 3]is a neurodegenerative disorder characterized by progressive loss of muscle control and coordination. This leads to variety of movement problems such as shaking of the limbs and head (tremors), muscle stiffness (rigidity), slowness in movement execution (Bradykinesia), difficulty with walking and impaired balance. Later in the course of the disease, cognitive and behavioral problems may arise. As symptoms worsen, it may become difficult to walk, talk, and complete simple tasks[1]. PD is more common in the elderly with most cases occurring after the age of 50 years. Sometimes PD occurs in younger adults. It affects both men and women.

Causes:

PD occurs when by some unknown causes, dopamine-producing nerve cells are slowly destroyed, which reduces dopamine levels in the parts of the brain. Dopamine acts as a chemical messenger between two brain areas - the substantia nigra and the corpus striatum - to produce smooth, controlled movements. When the amount of dopamine is too low, communication between them becomes ineffective impairing the movement. This leads to the loss of muscle function. The damage gets worse with time. Other cells in the brain also degenerate to some degree and may contribute to non-movement related symptoms of Parkinson's disease. The cause[4] of PD or dopamine destruction is still unknown but many researchers suspect it may be caused by a combination of genetic factors and environmental factors.

Symptoms:

1

The 3 key symptoms of Parkinsonism are tremor, bradykinesia and rigidity[5]. The disorder may affect one or both sides of the body. How much function is lost can vary. The symptoms of PD are mild at first and will progress over time. Characteristic motor symptoms include the following:

1. Tremors[6]: Tremor is an involuntary muscle contraction and relaxation of body parts, which includes trembling in fingers, hands, arms, feet, legs, jaw, or head. Tremors most often occur while the individual is resting. Tremors may worsen when an individual is excited, tired, or stressed.

2. Rigidity: Rigidity is the stiffness of the limbs and trunk, which may increase during movement[7]. It may produce muscle aches and pain. Rigidity results when there is an increase in muscle tone that causes resistance to passive movement throughout the whole range of motion.

3. Bradykinesia[8]: It is characterized by slowness of voluntary movement. Rather than being slowness in initiation (akinesia), bradykinesia describes slowness in the execution of movement. Over time, it may become difficult to initiate movement and to complete movement. Bradykinesia together with stiffness can also affect the facial muscles and result in an expressionless, "mask-like" appearance.

4. Postural instability

5. Parkinsonian gait

While the main symptoms of Parkinson's disease are movement-related, progressive loss of muscle control and continued damage to the brain can lead to secondary symptoms. These vary in severity, and not every individual will experience all of them. Some of the secondary symptoms include anxiety, insecurity, stress and increased sweating; confusion, memory loss,

2

and dementia; constipation; difficulty swallowing and excessive salivation; diminished sense of smell; skin problems; slowed, quieter speech, and monotone voice; and urinary urgency[1].

Diagnosis:

The diagnosis of PD is based on the patient's symptoms and a physical examination. A neurological exam may include an evaluation of coordination, walking, and fine motor tasks involving the hands. Several guidelines have been published to assist in the diagnosis of PD, which include the Unified Parkinson's Disease Rating Scale (UPDRS) [9, 10]. Tests are used to measure mental capacity, behavior, mood, daily living activities, and motor function. They can be very helpful in the initial diagnosis, to rule out other disorders, as well as in monitoring the progression of the disease to make therapeutic adjustments. Brain scans and other laboratory tests are also sometimes carried out, mostly to detect other disorders resembling Parkinson's disease.

The Unified Parkinson's Disease Rating Scale is a rating scale used to follow the longitudinal course of Parkinson's disease. The UPDRS has long been the major rating scale that is used to assess severity of symptoms of Parkinson's disease. The original version of the scale assessed daily activities, motor skills and mental capacity (including behavior and mood). When administering the scale, a neurologist observes your performance when moving your arms or legs or body and then scores your performance from 0 (normal) to 4 (severe). Therefore, the higher the UPDRS score, the greater the disability from PD. An updated version of the scale was recently developed by specialists from the Movement Disorder Society. The updated version adds new assessments of non-motor symptoms of PD. The UPDRS is a scale that was developed

3

as an effort to incorporate elements from existing scales to provide a comprehensive but efficient and flexible means to monitor PD-related disability and impairment

Treatment:

There is currently no treatment to cure Parkinson's disease. Several therapies are available to delay the onset of motor symptoms and to ameliorate motor symptoms. All of these therapies are designed to increase the amount of dopamine in the brain either by replacing dopamine, mimicking dopamine, or prolonging the effect of dopamine by inhibiting its breakdown. Studies have shown that early therapy in the non-motor stage can delay the onset of motor symptoms, thereby extending quality of life [11].

The most effective therapy for Parkinson's disease is levodopa (Sinemet), which is converted to dopamine in the brain. However, because long-term treatment with levodopa can lead to unpleasant side effects, its use is often delayed until motor impairment is more severe. In earlier stages of Parkinson's disease, substances that mimic the action of dopamine (dopamine agonists), and substances that reduce the breakdown of dopamine (monoamine oxidase type B (MAO-B) inhibitors) can be very efficacious in relieving motor symptoms. Unpleasant side effects of these preparations are quite common, including swelling caused by fluid accumulation in body tissues, drowsiness, constipation, dizziness, hallucinations, and nausea.

For some individuals with advanced, virtually unmanageable motor symptoms, surgery may be an option. In deep brain stimulation (DBS), the surgeon implants electrodes to stimulate areas of the brain involved in movement. In another type of surgery, specific areas in the brain that cause Parkinson's symptoms are destroyed.

In addition to medication and surgery, general lifestyle changes (rest and exercise), physical therapy, occupational therapy, and speech therapy may be beneficial.

4

1.2 Deep Brain Stimulation

DBS Techniques:

Deep brain stimulation (DBS) [12] is an established surgical procedure used to treat a variety of neurological symptoms, especially Parkinson's disease (PD) symptoms, such as tremor, rigidity, bradykinesia, slowed movement, and walking problems. At present, the procedure is used only for patients whose symptoms cannot be adequately controlled with medications. DBS uses a surgically implanted, battery-operated electro-medical device called a neurostimulator to deliver electrical stimulation to specified areas in the brain that control movement, blocking the abnormal nerve signals that cause PD symptoms.

Before the procedure, a neurosurgeon uses magnetic resonance imaging (MRI) or computed tomography (CT) scanning to identify and locate the exact target within the brain where electrical nerve signals generate the PD symptoms. Some surgeons also use microelectrode recording (MER), which involves a small wire that monitors the activity of nerve cells in the target area, to more specifically identify the precise brain target that will be stimulated. The DBS system consists of three components: the lead, the extension, and the neurostimulator. The lead or electrode is inserted through a small opening in the skull and implanted in the brain. The tip of the electrode is positioned within the targeted brain area. The extension is an insulated wire that is passed under the skin of the head, neck, and shoulder, connecting the lead to the neurostimulator. The neurostimulator (the "battery pack") is the third component and is usually implanted under the skin near the collarbone. In some cases it may be implanted lower in the chest or under the skin over the abdomen. Once the system is in place, electrical impulses are sent from the neurostimulator up along the extension wire and the lead and into the brain. These impulses interfere with and block the electrical signals that cause PD symptoms.

5

Ideal targets for DBS that shows clinical benefits and minimal adverse effect after stimulation through the DBS electrode are the thalamus, subthalamic nucleus, and globus pallidus.

Mechanism

DBS injects electrical charge into the brain, mediated by ions. The therapeutic benefit of DBS is related to adequate neuronal activation which requires generation of electrical impulse across the cell membrane and its transmission to next neuron. DBS tend to depolarize the cell membrane i.e. open the ion channels that create electric impulse to transmit. Many factors are involved in this activation and stimulation effect, which include the volume of brain stimulated and the number of neuronal elements activated within that volume. Generally, the volume of brain activated is related to the size of the electric field generated by DBS. The number of neuronal elements within the volume activated is related to the current density, which is the concentration of electrons (ions) within the electric field. We can manipulate the size of the electric field by adjusting the voltage and the combinations of active DBS contacts. We can manipulate the current densities within the electrical field by changing the configuration of the active DBS contacts. For example, monopolar stimulation where a single contact on the DBS lead acts as the cathode (negative contact) and the impulse generator case acts at the anode (positive contact) generates less concentrated current densities compared to bipolar where the anodes and cathodes are on the DBS lead.

Benefits and Risks of DBS:

Many PD symptoms including tremor, rigidity, bradykinesia and festinating gait shows significant improvement with DBS surgery. While symptoms like speech, dementia and state of

6

mind (depression, anxiety, obsessive or compulsive) may not improve or even worsen after DBS. Simultaneous attention needs to be given to these symptoms also. Patients with normal memory function show no significant post operative decline in most routine memory tests. However Patients with dementia however do experience a decline which may or may not represent the natural history of dementia

1.3 Brain Atlas [13]: Schaltenbrand-Wahren/Talairach-Tournoux brain atlas registration

Brain atlas is a number of records of human brain structure accompanied with coordinates used in study of brain anatomy. The digital atlas system provides several tools for registration, 3D display and real-time manipulation, object extraction/editing, quantification, image processing and analysis, reformatting, anatomical index operations, and file handling. The two main stereotactic atlases provided by the system are electronic and enhanced versions of Atlas of Stereotaxy of the Human Brain by Schaltenbrand and Wahren and Co-Planar Stereotactic Atlas of the Human Brain by Talairach and Tournoux.

1.4 Visual Representation of Clinical Scores and Description of Problem:

In case of DBS, the effects of electrical stimulation on PD symptoms are clinically scored on the basis of UPDRS. Each of the observed point recorded from various patients during the DBS surgery indicates the efficacy distribution of DBS in the brain. The visual representation of these clinical scores in the form of contour maps requires constructing a function which closely fits those data point. The superimposition of these functional contours over the anatomical brain atlas slides can help us locate the high yield anatomical regions which are functionally efficacious for DBS therapy. The major limitation is the loosely distributed data set. The unevenly distributed clinical data points with a low sampling density makes it difficult to model the function and

7

visualize it. Another challenge here is to measure the reliability of the developed model. Since the data set required to support the efficacy estimation of a particular location is very less, we are required to find methods to optimize the estimation and reliability of the interpolated model.

1.5 THESIS OVERVIEW:

Deep brain stimulation (DBS) is an established clinical therapeutic method for the treatment of movement disorders, especially for patients with advanced Parkinson's disease. The therapeutic effects of DBS are significant in alleviating Parkinsonian motor symptoms and reducing dependence on dopaminergic drugs. The subthalamic nucleus (STN) is accepted target for this procedure. However, researchers have found variations in efficacy and side-effects of DBS therapy within and around the STN. Various investigative groups have proposed diverse optimal sites for the stimulation in this region, which includes the dorsolateral parts of STN[14] [15], dorsal/dorsomedial to the STN in the region of the pallidofugal fibres, the caudal zona inceta (GILL), the preleminscal radiation (Velasco) and the rostral zona incerta (rZI) [14] [16] and at the junction between the dorsolateral part of the STN and the region dorsal/dorsomedial to it [17] [18] [19]. In addition to the debate about the optimal target within the STN region, variations within the patient population further complicate matters [20, 21]. Microeletrode recording (MER) is the gold standard in determining the anatomic location of an electrode and can reliably identify the motor portion of the STN. However, the proposition of other sites requires not only identification of the site by MER but also assessment of the effect of stimulation in these areas. Additionally the various cardinal symptoms of Parkinson's disease, namely tremor, rigidity, bradykinesia and voice status may differ in the location of their optimal treatment target. Considering these factors, it becomes necessary to study the functional effects of the DBS in a patient's population across all these target areas in order to optimize and evaluate various DBS

8

targets for each of the cardinal symptoms of PD. The improvement in patient's Parkinson's symptoms are qualitatively measured and scored during the DBS surgery by assessing the Unified Parkinson's Disease Rating Scale (UPDRS). In order to locate the optimal location of the DBS electrode, the surgeon needs to assess different electrode tracks and locations during the surgery. The location of the permanent electrode implantation is based upon the physiology assessed through MER and stimulation induced changes in the patient's PD symptoms as measured by the UPDRS during the DBS surgery. The change in UPDRS scores collected over number of patients for different Parkinsonian motor symptoms; along with the MER identified location of the electrode constitute a large database of dispersed AC-PC location in the STN region. This database of efficacy tied to anatomic and physiologic data obviously contains random variation and outliers making conclusions about efficacious areas difficult. Statistical analysis and modeling of efficacy distribution and variation in 3D space is required.

In this study, we will explore various interpolation methods and other analysis tools for the accurate spatial realization of this type of data. We will study 'Tessellation-based linear Delaunay triangulation interpolation', 'roving window interpolation' (RWI) [22] [23]and 'modified monopolar inverse distance weighted interpolation' technique (MIDW) in context of our data type. The other challenge is to statistically optimize the data set and measure the reliability and robustness of the constructed maps. The effect and performance of the estimator, i.e. the bootstrapping outcomes will be verified by Monte-Carlo's simulation.

Objective:

The overall objective of this study was to develop computational and analytical tools that help model the STN and surrounding region in the brain for their efficacy or side effects for DBS

therapy with respect to its boundaries and obtain an optimized topographical map of the brain region, reconstructed from clinical scores, based upon UPDRS. A systematic approach has been employed to develop the functional model, handle the variability issue, optimize the model and representation of the distribution contours. For instance for various interpolation techniques were studied and analyzed to find out the most appropriate technique that model the unique data-type with high predictability and accuracy. On the other hand various measures and tools are also explored and developed to handle the data variability and optimize the model.

Description of Chapters

This project involves developing various tools that facilitates better analysis of the DBS efficacy distribution and variations. Chapter 2 provides a brief description of the patient, surgical methods and data collected for analysis. Chapter 3 and 4 focus on the development of techniques for functional modeling and interpolation of the data points. Here chapter 3 deals with the general UPDRS data points while chapter 4 deals with the specialized requirement for different modeling techniques for monopolar and bipolar stimulation data sets. Chapter 5 focuses towards the different types of variability present in the database and techniques to measure and optimizes it in the model. Chapter 6 explains the additional tools and GUI that could help study the specific functional property of the region of interest. The statistically optimized and interpolated realizations were used to develop a functional model for DBS locations, with optimal reliability and accuracy. This will help DBS practitioners to locate the most promising site for stimulation.

A systematic step-by-step description of the methods is provided for each chapter. Additional details about the methods have been included separately in an Appendix at the end of the dissertation. A separate section in Appendix is dedicated to the user manual prepared for the

10

PDRG_GUI which facilitates endpoint users to easily study and analyze the DNS efficacy

distribution using the developed tools and techniques described in this paper.

11

This Chapter provides a brief description the patients, stereotactic and surgical method employed for DBS therapy and data collected for analysis. It also describes the calculation to change score values which serve as the functional data for the modeling in next chapters. At the end of the chapter a short description of the data distribution is given.

2.1. Surgical Methodology and Data Collection

During the placement of 69 deep brain stimulators in the subthalamic region for the treatment of Parkinson's disease, 657 points were evaluated for their MER identity and the effect of stimulation on the intraoperative UPDRS score. Surgeries were performed at the Medical College of Virginia Hospital (MCVH) or McGuire Veterans Affairs Medical Center using the CRW frame or a frameless stereotactic system (NexFrame).

The stereotactic target was identified on a MRI merged to a CT with either the CRW localizer or bone fiducials. All stereotactic targets and locations were described in relation to the midpoint of a line drawn from the midline of the anterior commissure (AC) and the midline of the posterior commissure (PC) after correction of roll, pitch, and yaw. The initial target for the subthalamic nucleus (STN) was 12 mm lateral, 4 mm posterior, and 4 mm deep to the mid AC-PC point.   A burr hole was created 2.5 - 3.5 cm off the midline anterior to the coronal suture. A cannula was placed through the stereotactic device and advanced into the brain. A microelectrode (ME) was then advanced with a microdrive to the target. Prior to the development of the MacroStim Interface (MSI) (FHC Inc., Bowdoinham, Me., USA), the ME was exchanged with the DBS for test stimulation. A bipolar configuration with the most distal contact being negative and next contact being positive at 3 volts was employed. After the introduction of the MSI,

12

macrostimulation was performed with the macro contact ring of the microelectrode. The MSI connects the Medtronic screener box (stimulation generator) to FHC's microTargeting™ differential recording electrodes, thus routing the current to the macro contact ring. In order to provide matching current density to the DBS, the MSI is set at 6 volts. Macrostimulation was conducted at a pulse width of 60 µs and 185 Hz at 2 mm intervals starting 10 mm above target and extending a variable distance below planned target depth.

Intraoperative efficacy assessment was based on change from baseline score on a modified Unified Parkinson Disease Rating Scale (UPDRS) scale as well as assessment of side effects at twice therapeutic voltage at the planned final depth.

A modified UPDRS score was obtained utilizing the components of the UPDRS that can be tested while the patient is on the operating table (see table x). Only the affected side is assessed. Change in subscores for tremor, rigidity, limb bradykinesia, and voice were calculated for each location. In addition the overall efficacy at each location was assessed as a percentage change from the baseline total score. The intraoperative macro-stimulation efficacy was determined by change from baseline UPDRS exam with stimulation and was expressed as a percentage.

 After MER and test stimulation, a conclusion was reached by the operative team as to the location of the electrode within the target region, and a decision was made to implant the DBS or move to another track. If another track was chosen, the direction and distance of the move was recorded. This process was repeated until the team felt that one of the tracks was located at an appropriate location. This decision was based on MER, macrostimulation efficacy, and a lack of significant macrostimulation-induced side effects at a low voltage. No attempt was made to fully

13

map the nucleus; the number of tracks was a reflection of the least number required to identify a therapeutic target.

Once a final track was chosen, the ME was replaced with the DBS lead. The lead was secured using the Medtronic burr hole cap or the StimLoc device (Image-Guided Neurologics, Inc. Melbourne, FL, US) (Medtronic, Inc., Minneapolis, Minn., USA) under fluoroscopic monitoring. At the end of the surgical procedure the patient was taken to the CT scanner and a CT at 1-2 mm intervals was obtained. This CT was then fused to the preoperative CT and MRI in the Stealth Station to obtain the AC-PC coordinates and angles of trajectory of the final DBS location.

The AC-PC coordinates and trajectory of the DBS lead is determined by post-operative imaging. The MER tract locations are then identified by their distance from the final trajectory. The AC-PC location of each stimulation point is calculated and each point is labeled as STN, SNR, or ZI based on the microelectrode sampling at that location.

2.2. Score Coordinates and Change Score Values:

The data obtained during the surgery (as explained above) are the intraoperative assessment of change in the clinical symptoms of Parkinson patients while undergoing DBS surgery. The clinical scores are the qualitative rating given by the surgeon and clinical staff during the surgery, by assessing the Unified Parkinson's Disease Rating Scale (UPDRS), while patients were receiving deep brain stimulation. Each of its components is rated on the scale of 0 (normal) to 4 (worst). These clinical sub-scores reflect improvement or worsening in one or more characteristic Parkinson disease's symptoms in the patient, which includes tremor, bradykinesia, rigidity and voice assessment. Each assessment is compared with the baseline score obtained without stimulation. The sum of various sub-scores obtained after stimulation at a particular spot in deep brain, reflects the overall efficacy and sensitivity of that location for DBS therapy. All

14

electrode positions were defined by their stereotactic Cartesian coordinates, referenced to the AC-PC midpoint (Schaltenbrand-Wahren Atlas). For each location stimulated, a clinical score is assigned to its location. The overall efficacy can be assessed as a percent change from the baseline score as represented by the following formula:

$$\text{Percentage Change Score}, P = \left(\frac{C_{base} - C_{score}}{C_{base}}\right) \times 100$$

Where C_{base} is the baseline value and C_{score} is the change score value.

In addition, change scores can be assessed for each symptom subscore, like

$$\text{Subscore Percentage Change Score}, P = \left(\frac{C_{SubS-base} - C_{SubS-score}}{C_{SubS-base}}\right) \times 100$$

2.3 Data Description and Categorization

This study involves the data obtained from 50+ patients during their DBS surgery, in past 10 years, in Medical College of Virginia, Richmond (VA) and VA Hospital, Richmond (VA). A total of 662 data points and their corresponding change score values were collected from above patients. Figure 1a and 1b shows the distribution of the change scores and percentage change scores in the database respectively. More the change score value of the data point more is the level of its efficacy towards the DB stimulation. Figure 2 shows the 3D distribution of the most efficacious data points (hot spots) for DBS in the ROI. Here the percentage change scores (Percch) of 70% or above are taken as the most efficacious (hot) observations. About 371 of the data points are from left side and 291 from right side of the brain. Anatomically, out of the 662 observations, 244 data points corresponds to the Sub-thalamic nuclei; 357, 50 and 11 data points corresponds to White matter, GPi and thalamus respectively. The region of interest is limited to a very specific region in brain defined in lateral direction [4 20] apc= [-14 6] and vertc= [-14 12].

15
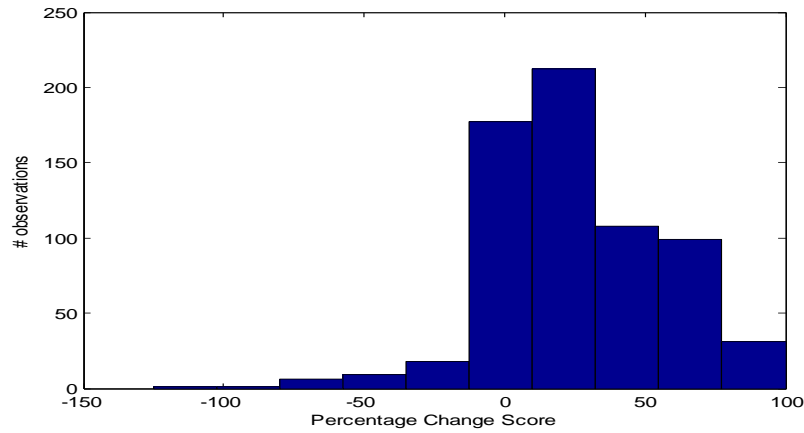
Figure 1: The distribution observation points of the and percentage change scores values in the

database

Figure 1 indicates that most of the data in the dataset has functional change scores in between 0

to 80%. Clinically the functional scores of more than 70% efficacy are considered as high

efficacy
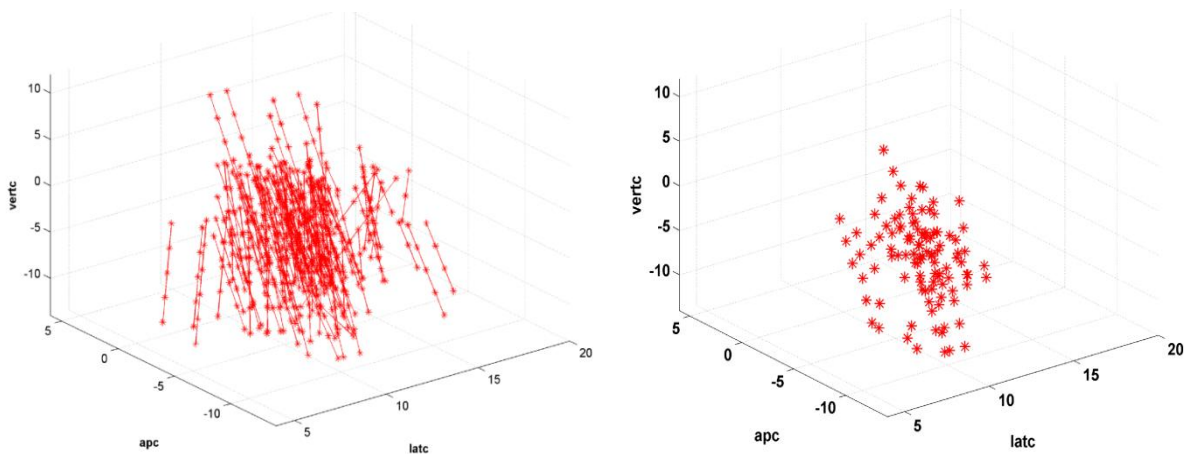
Figure 2: The 3 Dimensional distribution of the most efficacious data points (hot spots) for DBS
in the R.O.I. (percentage change scores $\geq$ 60%)

data. The final tracks have more efficacious data then rest of the tracks. Comparison of final

tracks and rest of the tracks, would provide an better understanding for track selection.

16

The sum of various sub-scores obtained after stimulation at a particular spot in deep brain, reflects the efficacy and sensitivity of that spot for DBS therapy. These spots are defined by their Cartesian coordinates, with respect to the AC-PC line (refer: SW Atlas). The obtained data can further be sub-categorized on the basis of anatomical location of the stimulating electrode; stimulation techniques (DBS and micro-canula based); tracks or passes into the brain on each side; and final tracks where electrodes are implanted permanently because of the identified efficacy

CHAPTER 3: Interpolations and Computational Modeling

INTRODUCTION

Background

Interpolation is a method of estimating functional values of new data points within the range of a discrete set of known data points by taking a weighted average of known functional values at these neighboring points. The output of sampling or experimentations in science and engineering yields functional values for a number of dispersed data points. The task of spatial interpolation is to construct a function that closely fits those points and approximate the functional values of the unexplored points. Fig 3.1 shows a simple example to understand interpolation method employed to model data points in 1D space. In this example (Mathworks, Natrick, MA), a signal is setup at y = [0 .5 1 1.5 2 1.5 1 .5 0 -.5 -1 -1.5 -2 -1.5 -1 -.5 0]; refer figure 3.a. Interpolation is then performed, using MATLAB 1D FFT interpolation function ' interpft', over this signal to produce other data points in the range of given data points, refer figure 3.b. Figure 4 shows interpolation applied in 2D and 3D space.
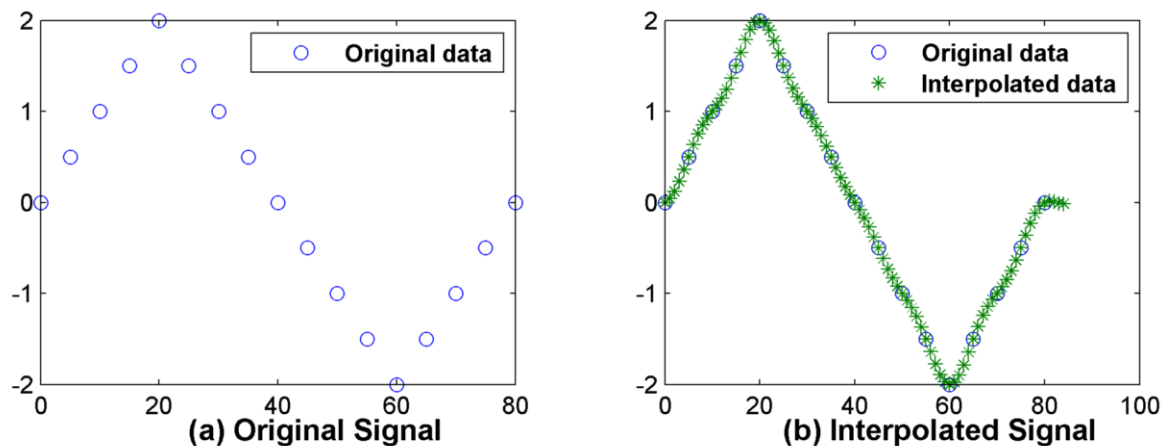
Figure 3: Interpolation in 1D. (a) Original signal; y (b) Interpolation over y.
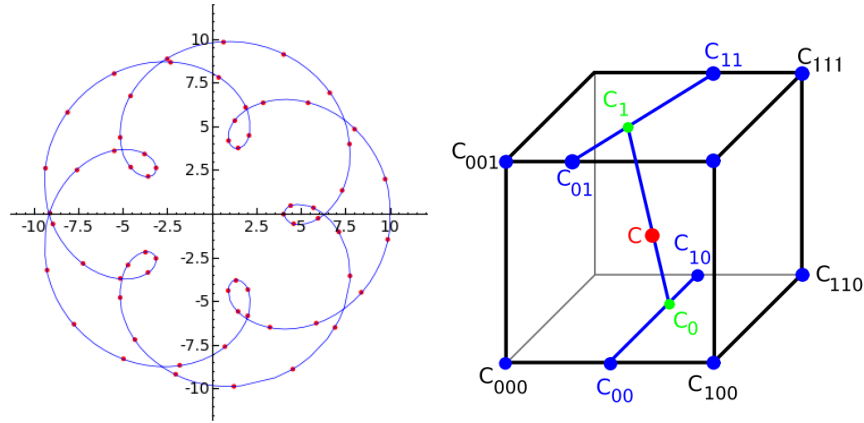
Figure 4: Interpolation applied in 2D and 3D space. *Source: en.wikipedia.org*

There are two main factors which govern the suitability of any interpolation technique in a particular discipline, namely, interpolation error and predictability. The interpolation tends to approximate a complex function (defining real spread of the functional values in ROI) by a simpler function, which yield an error depending upon the type of interpolation and level of assumptions. The interpolation methods having smaller interpolation errors produce smoother interpolants those are well fitted for the given data set, for instance polynomial interpolation are more smoother than linear one, but have increased complexity. Additionally, a method that fits well with some data can be unsuited for a different set of data points, or if measured in different locations of the same surface (Caruso). Hence, another criteria predictability or degree of prediction is important while considering interpolation reliability. The degree of prediction indicates the robustness of the produced model for new data sets.

There are many interpolation methods used to model randomly spaced point data. Some of the commonly used interpolation methods are linear triangulation interpolation, Inverse distance weighted method (IDW), Kriging, polynomial interpolation, tension finite difference method,

19

nearest triangle-based nearest neighbor interpolation, tetrahedron based linear interpolation, Hardy's interpolation, least square quadratic interpolation, or their modified forms. The selection of the most appropriate interpolation technique is based on the specific aim of the interpolation and the type and properties of the input data. Interpolation techniques utilizes various mathematical, physical and biological weighing factors to create the appropriate function, depending upon the type of data and the properties of the region. These factors may include electromagnetic field effects, impedance; geographical and environmental factors etc.

Applications to Interpolation: These various interpolation provides methods for transformation of values representing landscape phenomena measured at scattered points in a geographical region; 3D activation mapping in ventricular muscles; modeling biopotentials; image reconstruction from CT and MRI scans; texture synthesis; in digital signal processing, interpolation converts a sampled digital signal to a higher sampling rate using various digital filtering techniques.

Interpolation in DBS efficacy visualization:

For the visual representation of DBS clinical scores it is required to construct a function which closely fits those data point. Since the data type used to analyze the efficacy distribution and mapping is very unique, which consist of rating scores assigned to random scattered points in the ROI, the data analysis tools including the interpolation methods used to explore these efficacy scores haven't been studied systematically. In this study, we addressed this need by exploring and comparing various interpolation methods, effects of variation in various parameters involved in these methods and other analysis tools for the accurate spatial realization of this type of data. In general interpolation is a method of constructing new data points within the range of a discrete set of known data points. The objective of this study was to develop computational and analytical

tools that help model the STN and surrounding region in the brain for their efficacy or side effects for DBS therapy with respect to its boundaries and obtain an optimized topographical map of the brain region, reconstructed from clinical scores, based upon UPDRS.

In this study, we explored and compared various interpolation methods, effects of variation in various parameters involved in these methods and other analysis tools for the accurate spatial realization of this type of data. We studied 'Tessellation-based linear Delaunay triangulation interpolation', 'roving window interpolation' (RWI) [22] [23]and 'modified monopolar inverse distance weighted interpolation' technique (MIDW) in context of our data type. The MIDW interpolation technique is a modified form of RWI, developed on the basis of electric field geometry of the DBS monopolar electrode [24]. The developed model is intended to represent the high efficacy deep brain region, stimulation of which provides considerable improvement in PD symptoms.

METHODS

Interpolation Techniques

Three interpolation techniques for functional DBS mapping were investigated and the corresponding accuracy in estimating optimum efficacy level at unassigned locations within the ROI was evaluated. The techniques were the Tessellation-based 'linear Delaunay triangulation' interpolation, the 'Roving window' (RW) interpolation [22] and the modified monopolar Inverse-distance weighted method (MIDW) based on the point source approximation DBS model [24].

a. Tessellation-based 'Linear Delaunay Triangulation' Interpolation

2.4.1. Tessellation-based 'linear Delaunay triangulation' interpolation:

21

We used MATLAB griddata3 function which fits a hyper-surface of the form W = F(X,Y,Z) to the data in the (usually) nonuniformly-spaced vectors (X,Y,Z,V). GRIDDATA3 interpolates this hyper-surface at the points specified by (XI,YI, ZI) to produce three dimensional interpolation matrix, W. The method is based on Delaunay triangulation of the data that returns a set of simplices such that no data points are contained in any circumspheres of the simplices. The set of simplices forms the Delaunay tessellation. Then closest simplex is searched for the enclosing simplex of the Delaunay tessellation for each point in ROI. The function that defines the efficacy level at each point in ROI is given as:

$$Z_i(i) = p(i, :) \times (tri(t(i0, :)))$$

The purpose is to identify a neighborhood of nearby observation points to be used in the interpolation. Two options are available to perform the interpolation. The simplest method is a linear interpolation of the vertices of the triangulation. In this case, the barycentric coordinates of the point are used to take a weighted average of the three observation values (associated with the three vertices of the triangle). The resulting interpolation function is continuous, but not differentiable across an edge.
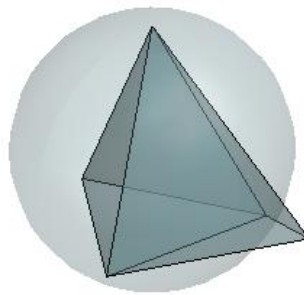

Figure: A 3-D Delaunay triangulation produces tetrahedra that satisfy the empty circumsphere criterion. Source: Mathworks, Natrick, MA

22

b. Roving window (RW) interpolation (Shenai et al.)

In this method, the whole ROI is modeled as a 41 X 33 X53 point grid system which divides it into 71709 voxels of size 0.125 cubic mm (0.5X0.5x0.5). Here the 3D region was selected to encompass the STN, GPI and the white matter around it. point grid, with points (x_i, y_j) is constructed in the AC-PC plane of interest at $z = Z$ (the numerical instance along the vertical coordinate, z). A 3-dimensional iterative process is executed, with each point (x_i, y_j, z_i) serving as the center of a mathematical sphere with radius (r) = 2 mm. At each of these points the observations are searched from the databases that are contained within this sphere centered at the particular grid point. The change score values of these observations are averaged and saved as 'mean (v)'. The assignment of the final scores for that point is calculated on the basis of following function:

Z_i =   mean (v) ;   if number of observations found within the sphere is greater than or equal to
            5 AND standard deviation of the change scores of these observations are
            less than 1.5.

       No score;   else

c. MIDW Interpolation Techniques

The MIDW interpolation method is similar to the RW interpolation method except that the inverse distance- weighted score is assigned to the selected grid point instead of the simple average of the score values of the observation points within the sphere. The sphere surrounding the point location, where the new interpolated score needs to be calculated, is termed as search window with radius 'r'.

The algorithm employed for the MIDW interpolation is as follows:-

23

1. The whole ROI was modeled as a 41 X 33 X53 point grid system which divided it into 71709 voxels of size 0.125 cubic mm (0.5X0.5x0.5 mm^3), in which the 3D region was selected to encompass the STN, thalamus and the white matter around STN.

2. At each of these grid points in the ROI, the observation points were searched from the point centered at the selected grid in a sphere (search window) with the radius, r = 2 mm in the databases.

3. Each observation points present in the search window contribute its efficacy effect at the selected interpolant point by inverse distance weight [25-27]. Here, the property at each unknown interpolant location for which a solution is sought is given by:

$$P_i = \frac{\sum_{j=1}^{G} \frac{P_j}{D_{ij}^n}}{\sum_{j=1}^{G} \frac{1}{D_{ij}^n}}$$

Where P_i is the efficacy score calculated at interpolant location i given by coordinate (x_i, y_i, z_i) ; P_j is the change score value at sampled location j; D_{ij} is the distance from the point location i to the point location j; G is the number of sampled locations (those which are within the sphere centered at point location i); and n is the inverse-distance weighting power.

4. Repeated calculated for all the grid points in R.O.I.

5. The output of the above 3D iterative process is the estimate of DBS efficacy distribution in the ROI. The produced interpolations were than visualized using MATLAB 2D plotting function 'counterf' providing a 2D map of the selected plane in ROI.

The two important varying parameters involved in the calculations of MIDW interpolation were the search window radius (r) and inverse-distance weighting power (n). The inverse-distance

24

weighting power is the exponent of inverse distance (D) in MIDW formula (step 3 above). The weighting power defines the rate at which weights fall off with distance between the interpolated and the sample locations. A typical value of range is 1-4. To analyze the effect of both of these parameters we performed MIDW interpolation of the dataset using the combinations of 'r' and 'n'. Then we compared their interpolation errors and predictability to deduce the optimum combination for suitable realization.

The value of n, in effect, controls the region of influence of each of the sampled locations. As n increases, the region of influence decreases until, in the limit, it becomes the area which is closer to point I than to any other. When n is set equal to zero, the method is identical to simply averaging the sampled values. As n gets larger, the method approximates the Voronoi tessellation procedure (Watson and Philip, 1985). Usually, the value of n is set arbitrarily. Values of 1.65 and 2 were used for n by Kelway (1974) and NOAA (1972), respectively, for interpolating rainfall, while the ARMOS model (Kaluarachchi et al., 1990) recommends the use of values ranging from 4 to 8 for interpolating oil pressure heads.

(a)Result of searching observation points in search window

(b)Efficacy Distribution due to Single Electrode Stimulation
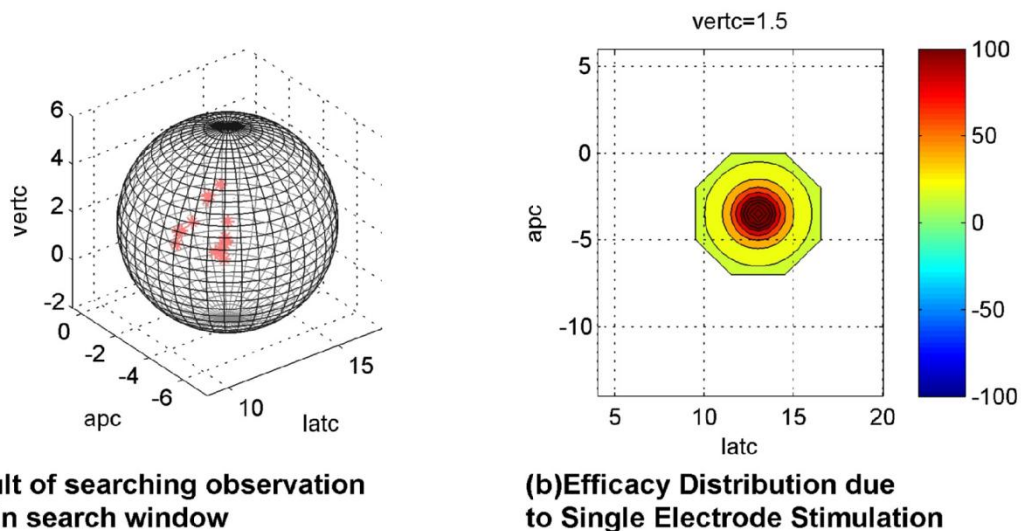
Figure: (a)Result of searching observation points in search window (b)Efficacy Distribution due to Single Electrode Stimulation'

Comparison of the performance interpolation methods

The performance of the interpolation method was characterized by the normalized interpolation errors, i.e. the normalized root mean square error [28] for the interpolation:

$$\text{Normalized RMSE} = \frac{\sqrt{\frac{\sum_{i=1}^{N}(V_R - W_I)^2}{N}}}{Rn}$$

Where V_R is the observed sample value and W_I is the interpolated value at a selected coordinate point in ROI. N is the number of the observation points and Rn is the range of score values (in case of percentage change value, Range = (100 – (-100)) = 200).

Cross-Validation of Developed Model: Find out Predictability of the interpolation method.

The robustness of the investigated interpolated methods was evaluated by the cross-validation methods. The 'Leave one patient out cross-validation' (LPOCV) and 'Leave one observation out cross-validation' (LOCV) ([29], Andrew and W. Moore) techniques were employed. For LPOCV, a single patient was arbitrarily selected and all his/her related observations were temporarily removed from the dataset. The rest of the dataset was used to construct the interpolations using the interpolation methods employed. The models then were cross-validated using the data from the excluded patient. The above process was repeated for every patient and the mean error was measured. Similarly, for LOCV, one observation was left out from the whole data set and the rest data was used to interpolate. The left out observation was used to cross-validate. This procedure was repeated for every observation in the dataset.

The performance to cross-validation was measured by the degree of prediction of the constructed mathematical model with respect to the new or the excluded data. The predictability or the degree of prediction of the interpolated model was determined by the expected variance denoted by R^2 [30]. The more the R^2 is near to 1, better the calculated data fits the measured one.

26

$$\text{Degree of Prediction, } R^2 = 1 - \frac{\sum_N (w_i - V_R)^2}{\sum_N (V_R - V_{AV})^2}$$

Where V_R is the observed sample value and w_i is the interpolated value at a coordinate point in ROI; V_{AV} is the average of all observations.

RESULTS
Interpolations of Data

Figure 1depicts the contour maps constructed from the 3 different interpolation techniques, namely Tessellation-based 'linear Delaunay triangulation' interpolation (fig. 1a,d,g), 'Roving window' interpolation (fig. 1-b,e,h) and Monopolar Inverse-distance weighted interpolation (fig. 1-c,f,i) in lateral (fig. 1-a,b,c), coronal (fig. 1-d,e,f) and transverse planes (fig. 1-g,h,i). The figures 1-c,f,i shows the contour maps produced using MIDW interpolation method with search window radius 2 mm and power of inverse distance as 3.

We can easily locate the red spot in lateral plane, near point (-3, -5) in all three interpolation realizations. The presence of poor efficacy spot (blue spot) at (-5,-5) is most prominent in Linear triangulation map, a little faded in MIDW map, but almost absent in RW map. The extent of the map boundaries (region covered) is more in RW and MIDW interpolations than Triangulation interpolation. Also, from transverse plane maps, the triangulation and MIDW maps show gradual gradation of hot and poor spots which helps locating the center of major spots.
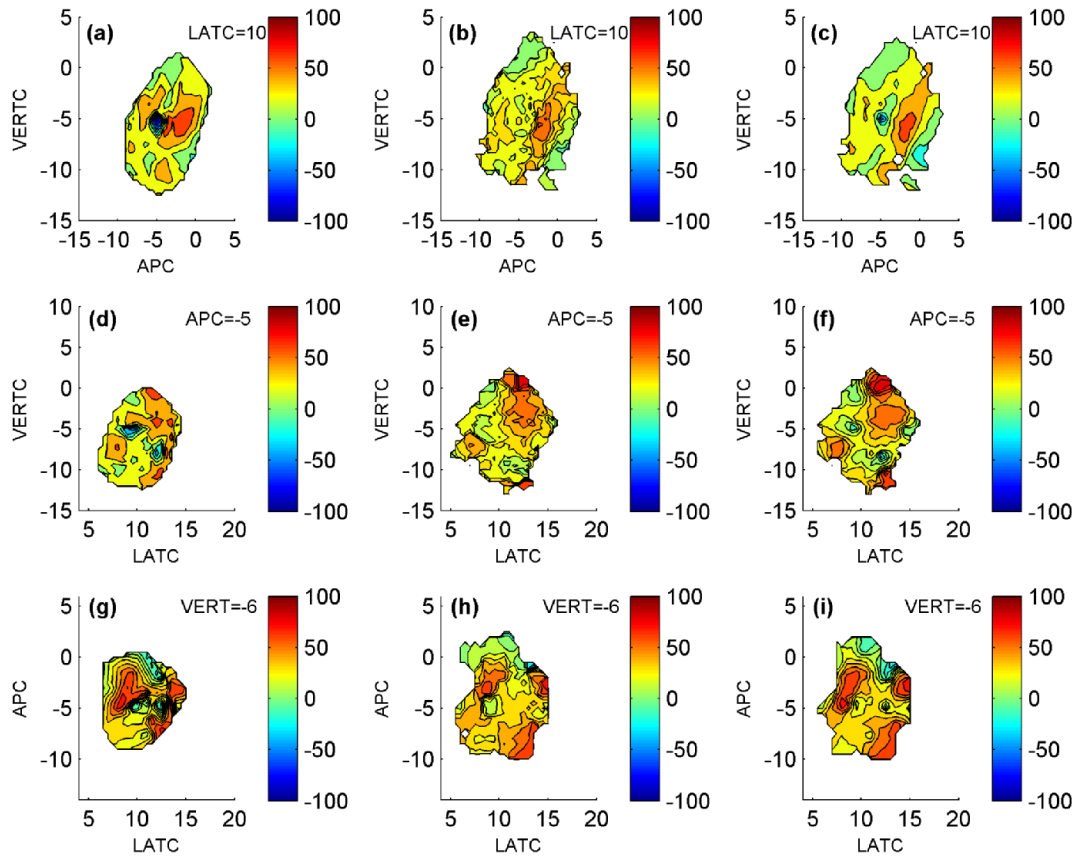
Figure 5: the contour plots comparing the three interpolation techniques on three different planes. Figure 1a-b-c, 1d-e-f and 1g-h-i shows the interpolated contour plots in lateral plane at a coordinate point 8 mm right from the center of AC-PC, coronal plane at a coordinate point 10 mm posterior to the AC-PC and transverse plane at a coordinate point 4 mm inferior to the AC-PC respectively . Figure 1a shows the Triangulation interpolation, Figure 1b shows the Roving window maps and figure 1c shows the MIDW contours for monopolar stimulation. The percentage change in score value (or percentage efficacy) are represented by color bars, where dark red color indicates the highest efficacy region (hot spot) while blue color shows poor efficacy towards DBS.

Comparison of Interpolation Methods and Interpolation Errors

Table 1 depicts the results of comparison among 3 different interpolation methods described

above. First column shows the Normalized root mean square error for the above categories

whereas the second column depicts the interpolation error with respect to the original value. The

28

results are shown for two different categories of datasets. First the entire dataset of all the patients who had undergone DBS is used for modeling and error calculation. Secondly, the part of monopolar DBS dataset is considered which is collected from subthalamic nucleus only. For both the dataset groups, there is sufficient evidence that the Linear Triangulation interpolation method models the database with better accuracy than RW interpolation. However, MIDW interpolation with optimized parameter values (r=2 mm, r^3) shows much improved accuracy as compared to LT and RW method. Additionally, the interpolation errors were less when observations from only STN are modeled.

Table 1

Interpolation Errors

	Normalized Root Mean Square Error (RMSE)		
Data	**Modified MIDW (D^3)**	**Linear Triangulation**	**Roving Window Interpolation**
Entire data	0.0903	0.1219	0.3006
Data from STN region.	0.0913	0.1943	0.3032

Table 2 shows the effect of varying parameters the search window radius (r) on the interpolation accuracy. The roving window technique is shown as a case of MIDW Interpolation where inverse distance weight has zero power. Linear Triangulation results are also included for reference. From these comparisons and by observing the continuum of the produced maps in each case (reference my thesis) the optimum search window radius is found to be 2 mm. As we reduce the radius, the interpolation error reduces to a nadir at 2mm and then it increases slightly at 1mm. Table 3 shows the effect of varying power parameter of inverse distance weight in

29

MIDW interpolation method. A value of 1-4 is typical for the power factor. It is found that as the

power factor increases the accuracy of the interpolation increases.

Table 2

Effect of varying radius in MIDWI:

Normalized RMSE

Data	Triangulation	RW I	MIDW (varying radius of search window) for r^2.			
	--	--	r =1	r =2	r =3	r = 4
Entire data	0.1219	0.3006	0.1323	0.1297	0.1459	0.1581
Data from STN	0.1943	0.3032	0.1296	0.1267	0.1324	0.1394

Table 3

Effect of varying power of inverse distance weight in MIDWI:

Normalized RMSE

Data	Trian- gulation	Roving Window	Modified MIDW (varying power of inverse distance) for r = 2mm		
	--	D^0	D	D^2	D^3
Entire data	0.1219	0.3006	0.2140	0.1304	0.0903
Data from STN region.	0.1943	0.3032	0.2170	0.1274	0.0913

Table 4 depicts the result of cross validation (in terms of predictability for new set of

observations) of the above described interpolation methods with varying parameters in case of

MIDW interpolation. It is found that Linear Triangulation interpolation method has the best

30

predictability (nearer to 1) as compared to any other interpolation method, in both the data

categories. The MIDW has better predictability than RW method.

Table 4

Cross Validation: Degree of Prediction

Prediction R^2 (Expected Variance or degree of Prediction)								
Leave one patient out CV								
Data	Trian-gulation	Roving window	Modified Monopolar (varying power parameter of inverse distance)			Modified Monopolar (varying radius of search window) for r^2.		
		D^0	D	D^2	D^3	r =1	r =2	r =3	r = 4
Entire data	0.2986	0.0367	0.0441	0.0822	0.1420	0.0535	0.0822	0.0437	0.0447
Data from STN	0.7629	0.2768	0.3151	0.4056	0.5088	0.2320	0.4056	0.1216	0.1456
Leave one observation out CV								
	Triangulation		Mahesh (RW)		Modified Monopolar Interpolation (r^3)			
Entire data	-0.2032		-0.0460		-0.1492			

Figure 2a shows a plot of Interpolation Error and predictability as a function of power of inverse

distance weight in MIDW interpolation method. From this graph, as the power increases from

the factor of 3, the increment slope in predictability and decrement slope of interpolation error

both tends to become straight. Thus, power factor of 3 can be considered as optimum in case of

MIDW interpolation. Figure 2b shows a plot of Interpolation Error and predictability as a

function of radius of search window in MIDW interpolation method. From this graph, it is clear

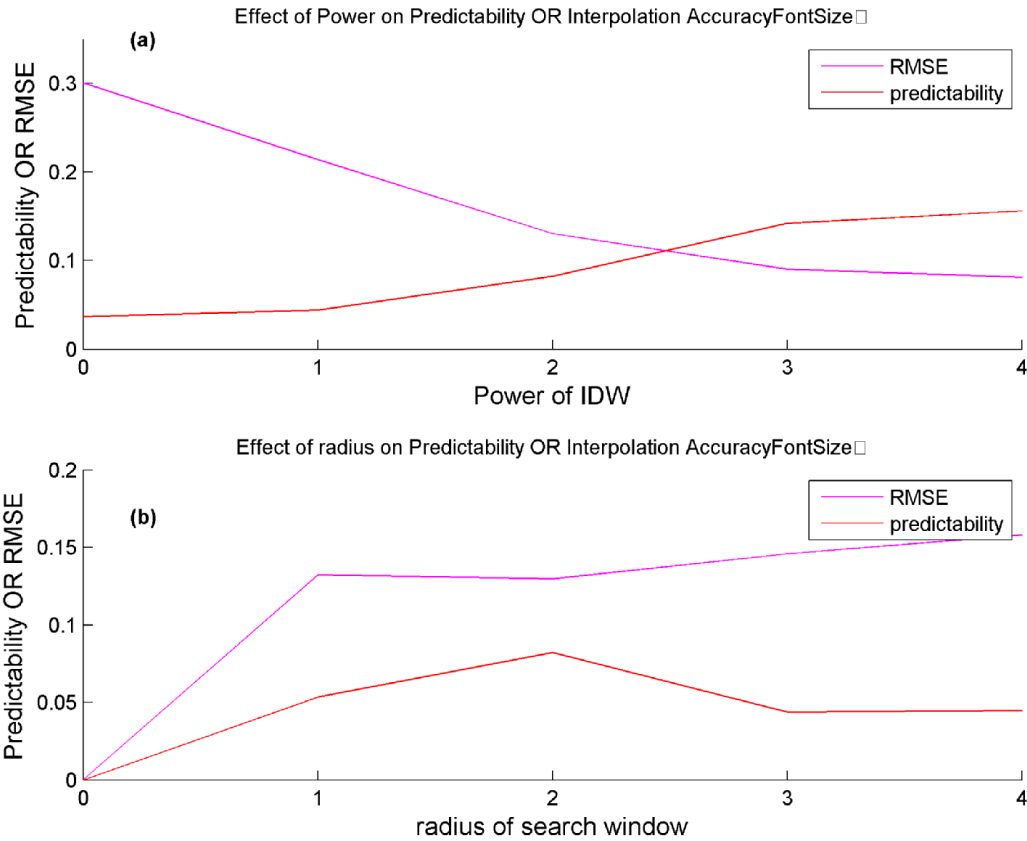that the optimum search radius is at r = 2mm.

31

Figure 6. (a) Predictability and RMSE versus Power of IDW; (b) Predictability and RMSE

Versus radius of search window

DISCUSSION:

This study indicates that the MIDW interpolation is most suitable technique to model the DBS

efficacy among the explored methods, in terms of a balance between interpolation accuracy,

predictability and electro-physical considerations. This methodology was used to create a visual

representation of DBS efficacy distribution by constructing a function which closely models the

efficacy levels of previously observed data point and generate a reliable and robust estimation for

new locations in the ROI.

Since the data type used to analyze the efficacy distribution and mapping is very unique, which

consist of rating scores assigned (efficacy for DBS) to random scattered points in the ROI, the

32

data analysis tools including the interpolation methods used to explore these efficacy scores haven't been studied systematically. This type of data needs suitable interpolation tools that fit the requirements to construct new data points within the range of a discrete set of known data points. Tessellation-based 'linear Delaunay triangulation' interpolation is an established technique for interpolation that proved to be a well suited for estimating new data points where the known data points are randomly scattered in the ROI. It fits a hyper-surface in the non-uniformly spaced vectors and interpolates this hyper-surface to produce three dimensional interpolation matrixes. It shows an acceptable predictability (R^2 = 0.2986 for entire ROI and R^2 = 0.7629 for the sub-thalamic nucleus) and accuracy (Normalized RMSE = 0.1219 and 0.1943 for entire ROI and the sub-thalamic nucleus respectively). However, this technique has limitation of inability to correctly interpolate concave objects [31]. Additionally, it doesn't consider representation of ROI in terms of the distribution of electrical potential of the DB stimulation. [32] and [31] used linear triangulation along with surface smoothing techniques like mesh cubes (also used in [33]), but to develop deformable brain atlas modeling the anatomical sub-structures. Due to the fact that MIDW interpolation considers the electric field geometry and has better interpolation accuracy (Normalized RMSE = 0.0903 and 0.0913 for entire ROI and the sub-thalamic nucleus respectively), MIDW also proves to be a reliable tool for analysis. IDW interpolation was used previously in [34] to develop a continuous and smooth variation maps on sampling data. Considering the effect of varying power of radius, the interpolation error (Normalized RMSE) and the degree of prediction (R^2) becomes better as the power increases. Similarly, if the radius of activation sphere around the point is varied, the optimum radius comes out to be r = 2 mm. Increasing or decreasing radius from 2 mm, results in worst output. The roving window interpolation method [22] [35] also analyzes the collection of neighboring data

points around the interpolant points, but do not consider the effect of distance from the stimulation spot on the tissue activation.

The MIDW interpolation is a modification of roving window technique which tends to exploits the electric field geometry of the stimulating electrodes [22]. The UPDRS value at a stimulation spot indicates the efficacy level of that spot for DBS therapy in terms of improvement in PD symptoms. The functional configuration of this spot and its surrounding region is based on the activation field generated by the DBS electrodes during the stimulation. The tissues present at the electrode-tissue interface experience significant electric field effect which shows the relevant improvement in the external PD symptoms. However as the distance from the electrode increases, the strength of electric field and thus the tissue activation level reduces (inverse square proportionality), and so the contribution of far tissues toward the observed improvement (or worsening). Hence, a high UPDRS value (considerable improvement in PD symptoms) at a particular spot in the brain demonstrates high sensitivity of the tissues present at that spot for DBS therapy which decreases as we move away from the spot. MIDW Interpolation method is adapted based on the of point source approximation DBS model of monopolar cathodic stimulation of brain tissues [24]. Although, factors like tissue impedance and conductivity, internal neuronal connections and anatomical inconsistencies were not considered in the model. The roving window and MIDW interpolation methods open the path towards development of better modeling techniques for the DBS efficacy, with lesser processing time [35].

34

CHAPTER 4: Monopolar and Bipolar DBS Modeling

Introduction

The therapeutic efficacy of DBS in PD is associated with the appropriate activation of neuronal elements, which depend upon the volume of stimulated region and number of neuronal elements activated within that region (Montgomery). These factors are related with the size of electric field and current density within the stimulated region respectively and can be manipulated by controlling DBS voltage and configuring active DBS contacts. By controlling the voltage and electrode configurations, an enormous number of electric fields can be generated with different sizes and strengths. This has the advantages of allowing the DBS electrical field to be tailored to the unique regional anatomy of each patient and the unique relationship of the DBS lead to the patient's regional anatomy.

The monopolar and bipolar DBS generate different electric field in the deep brain tissues and thus activate them in different manner. In order to get a better picture of the scenario, we need to analyze both the data type altogether, handling them with different interpolation techniques, that mathematically and electrostatically fit their activation geometry. The proposed adaptive interpolation technique appropriately maps the efficacy level of the entire region of interest and functionally models the hot spots for DBS therapy.

Monopolar versus Bipolar DBS

Monopolar and bipolar are the two possible electrode configurations used in DBS therapy. Monopolar stimulation where a single contact on the DBS lead acts as the cathode (negative contact) and the impulse generator case acts at the anode (positive contact) generates less

35

concentrated current densities compared to bipolar where the anodes and cathodes are on the DBS lead. The monopolar and bipolar DBS creates different electric field in the deep brain tissues. In the case of monopolar DBS, the lines of electrical force radiate outwards from the cathode on the DBS lead and the activation region (~ isosurfaces) around the electrode are concentric spheres equidistance from the electrode location. The strength of electric field (effect) decreases (inverse proportionality) as we go away from the source. The effect of DBS (UPDRS scores) at any stimulation spot indicates the efficacy level of that spot for DBS. This also indicates the activation level of the spot and the surrounding tissues, which decreases with the distance from the electrode location. the factors like tissue impedance, regional anatomy, orientation plays important role in formation of activation region around the electrode. On the other hand, bipolar stimulation creates electric field lines radiating from positive electrode to the negative one, forming an elliptical shape. The system generates isosurfaces around each electrode (positive and negative), depending upon its strength and the distance between the two electrodes. monopolar stimulation the widest spread of the electrical field at the same relative voltages than bipolar DBS.
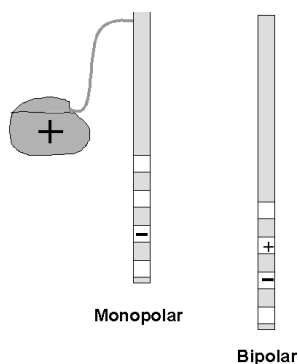

Figure 7. monopolar and bipolar electrode leads

Specifications and configurations of DBS leads: commercially available Medtronic DBS lead 3387 and 3389 specifications: (Medtronic model 3387, Medtronic Inc., Minneapolis, MN)

1. Distance from tip to electrode 'o' positions (which I guess is the negative electrode) is (1.5+1) ~ 2.5 mm.
2. Similarly distance from tip to electrode '1' position (Positive Electrode) is ~ 5 mm (4 mm in case of 3389).
3. If we consider that the negative electrode has larger amplitude we can approximate the location of activation centre in this case to be ~ 2.22mm from the tip data.
4. However, more realistically we can consider the activation centre to be somewhere in between the large negative and small positive electrodes, which comes out to be ~ 3.75 mm (for 3387) or ~ 3.2 mm (for 3379).

Figure 8. Medtronic DBS lead 3387 and 3389.
Source: ttp://professional.medtronic.com/products/

Concept of Inverse Distance Modeling:

This technique explores the electric field geometry of the stimulating source. The UPDRS score at a stimulation spot indicates the efficacy level of that spot for DBS therapy in terms of improvement in PD symptoms. The functional configuration of this spot and its surrounding region is based on the activation field generated by the DBS electrodes during the stimulation. The tissues present at the electrode-tissue interface experience significant electric field effect which shows the relevant improvement in the external PD symptoms. However as the distance from the electrode increases, the strength of electric field and thus the tissue activation level reduces (inverse distance proportionality), and so the contribution of far tissues toward the

observed improvement (or worsening). Hence, a high UPDRS value (considerable improvement in PD symptoms) at a particular spot in the brain demonstrates high sensitivity of the tissues present at that spot for DBS therapy which decreases as we move away from the spot.

Monopolar Vs Bipolar Stimulation Modeling:

Monopolar Interpolation method is based on the of point source approximation DBS model of monopolar cathodic stimulation of brain tissues (Zhang and Grill). The stimulation spot is considered as a monopole and the corresponding efficacy distribution is calculated based upon the inverse weighted distance interpolation method (Lam, 1983). However, in case of bipolar stimulation, the electric field effect and thus the activation geometry are different than that of monopolar. The stimulation spot is model as 2 separate monopoles. The system generates isosurfaces around each of the monopole (positive and negative), depending upon its strength. The resultant efficacy at a point location is the weighted efficacy due to the combined dipole. The calculation of weight factor here is based upon the vector resultant of the activation level (or the electric field) of the two monopoles at that point. The weight factor considers both the distance and orientation of dipoles with respect to the point location.

METHODS
Monopolar Versus Bipolar Inverse Distance weighted Interpolation techniques.

Compensation of the effect of mono-polar and bipolar electrode stimulation techniques.

In order to compensate the difference in activation region and iso-surface produced by

monopolar and bipolar stimulations with respect to their electrode tip location respectively, we

tried the following separate interpolation techniques. Detail description of the interpolation are

as follows:-

For Bipolar simulation Interpolation:

1. Consider a point in the meshgrid

2. For each point in the region of Interest, search for bipolar observation points located

    within a sphere of radius 2 mm around the selected point.

3. For each of them locate the positive and negative electrode coordinates.

4. Locate the midpoints of the dipoles and the distance of selected point from them and the

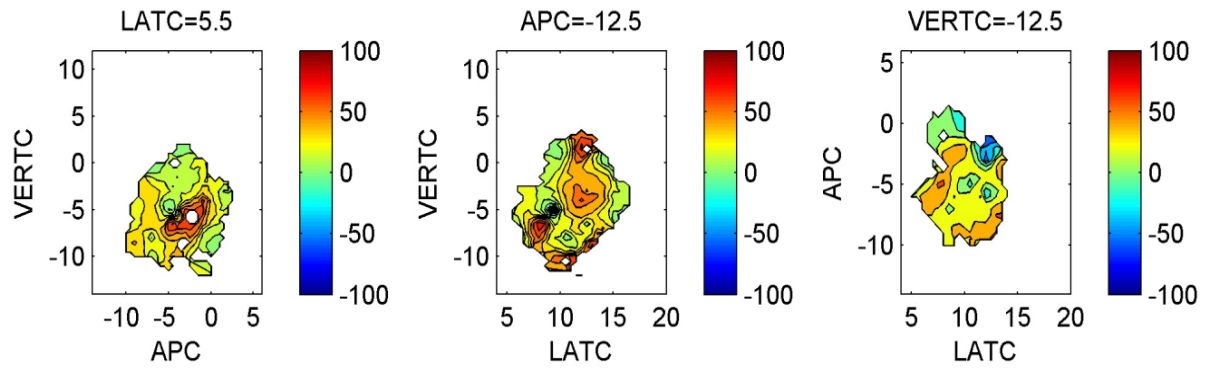   angle it makes with the dipole axis.

Fig. 2.2
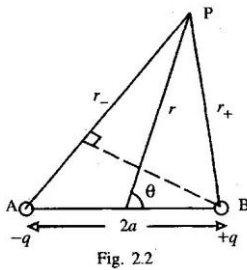
5. Calculate EF dues to these dipoles at the selected point. Take the mean of all the values.

$$\text{Activation contribution} \propto \frac{V\,(1 + 3\cos\theta)}{r^3}$$
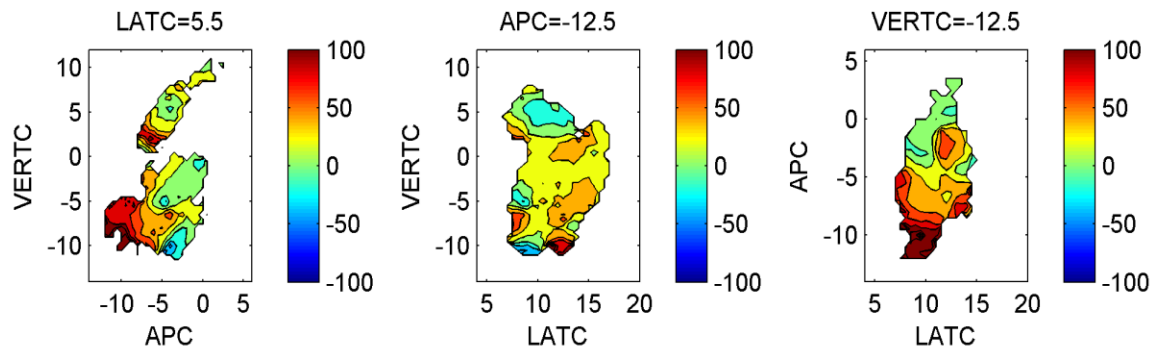
Where, V = score value.

6. This is calculated for all the points in R.O.I.

7. Apply boundary conditions.

39

RESULTS

(a) Monopolar Interpolation

(b) Bipolar Interpolation

Figure 9: monopolar VS bipolar interpolation

DISCUSSION

A differential interpolation technique is developed that can treat appropriately treat the data on the basis of stimulation type, namely monopolar and bipolar stimulation. The two types of electrode stimulations, monopolar and bipolar stimulations generate different type of electric field in the neighboring tissues and thus activate/ affect them in different manner. In order to get a better picture of the scenario, we tried to analyze both the data type altogether, handling them with different interpolation techniques, that mathematically and electrostatically fit their activation geometry. The proposed mapping technique offers a scheme to appropriately map the efficacy level of the whole region of interest and functionally model the hot spots for DBS therapy.

The activation region (isosurfaces) around the monopolar stimulation electrodes is the concentric spheres equidistance from the electrode location. On the other hand, the electric field due uneven bipolar stimulation and the activation region for these electrodes are different [24]. The system generates isosurfaces around each electrode (positive and negative), depending upon its strength. Since the activation region and electric field produced by both Monopolar and Bipolar stimulations are different, we need to employing different interpolation techniques for both. These interpolation techniques take under consideration the fact about isosurface and activation region for both the devices. In this paper we also discuss the possibility of an adaptive interpolation techniques developed to appropriately model these two different modes of DBS

CHAPTER 5: Variability and Statistical Optimization

INTRODUCTION

Variability is the tendency of the measurement process to produce slightly different data on the same test item, where conditions of measurement are either stable or vary over time, individual patient, technique, or the location. In this study, we considered variability issues like the observational variability (observation, tracks), inter-patient variability, sub-score variability (i.e. variations in efficacy regions of PD symptoms: tremor, rigidity, bradykinesia , voice and overall score) and variability due to stimulation parameters (monopolar DBS versus bipolar DBS). The measure of precision is a standard deviation. Good precision implies a small standard deviation. Here we will try to come up with a formula to develop the error model estimator that would include several error components and their variability measures.

We dealt with this variability in following ways:-

1. Variation in the efficacy distribution in the created models using monopolar and bipolar DBS database separately, were due to the different activation regions created by both the devices. This variability was reduced by employing different interpolation techniques used to model them separately (discussed in section 4).

2. The observational and inter-patient variability: To measure and reduce the effect of this variability, we employed bootstrapping based optimization to the interpolation or modeling techniques (discussed in section 5.2)

3. The variability among various PD symptoms and anatomical locations have clinical significance and is an important criteria for future studies. The visualization tools and the

42

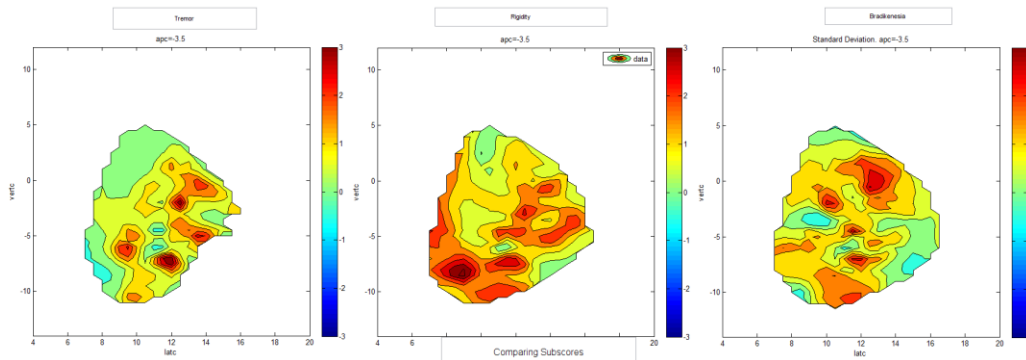Graphic User Interface described in Chapter 6 assist in exploring and comparing these spatial variability.

Figure 11.Contours comparing efficacy distribution of PD symptoms

Bootstrapping based optimization and Types

In order to check the robustness of our interpolated maps and model, we employed bootstrapping technique by randomly selecting samples from our observations to form thousand new sets of data for interpolation and mapping. Around each region, with higher mean change score values, a confidence interval is created by adding the standard deviation to the voxel mean value. This confidence region around the selected voxel, shows the region of agreement, where the effect of DBS therapy is likely to be efficient. Type of bootstrapping: patient-wise & observation wise: In order to study and measure the observational variability and inter-patient variability, two different type of bootstrapping based optimization techniques were employed.

The objective of this study was to use bootstrapping based optimization to reduce the effect of outlier data that mislead the realization in case of direct interpolation and enhance the reliability of the produced model. The optimization of the functional model is needed to make the constructed maps more effective and reliable

METHODS

43

Bootstrapping Based Optimization

For bootstrapping, we adapted two different techniques to assess the variance of the interpolated efficacy distribution of DBS spots: observation-wise bootstrapping and patient-wise bootstrapping. In the first technique, we obtained thousand new sets of data by randomly selecting Nu observations from our database (Nu is the size of observed dataset) for each dataset and then performing interpolation to obtain the 3D model for each. Similarly, for latter, we obtained thousand new sets of data by randomly selecting patients and the data obtained from them, until the number of observations equals the size of original dataset. Interpolation is performed for each of the bootstrapped dataset obtained above.

The whole region of interest (ROI) for the DBS was theoretically divided into a set of equal voxels (0.5mm ×0.5 mm ×0.5mm) and each voxel was correspondingly assigned an efficacy score based on the outcomes of the interpolation. For each voxel of the ROI we calculated mean and standard deviation of the 1000 bootstrapped interpolations. The set of means of all voxels now represents the estimate of the spatial distribution of efficacy level of the DBS targeted ROI. The mean contour plots, obtained from bootstrapping, produced at different planes, are the estimator of the true efficacy level of that region. Another three dimensional realization of the ROI is produced using the variance of the mean of each voxel bootstrapped mean (Standard Error of the mean). This indicates the degree of the reliability of the assigned efficacy level of the specific mass of the ROI.

Simulation: Validate the Performance of Optimization

44

A computer intensive simulation was performed to assess the performance of the bootstrapping optimization techniques employed in this study. The simulated data type and the structure of the 3D region were similar to the real data and the considered region of interest. This simulation study involves creating a 3D model of a region similar to that of the region under study and generating several independent data sets that assign score values to randomly selected points in the specified region (with the help of random number generator in MATLAB). An arbitrary portion within the ROI was allocated as high efficacy region. Similarly, a different portion was allotted for outlier observations (small number of observations, 48). Outlier data here are high efficacy observations that reside at a location other than actual hot spot. It represents err data produced due to experimental or patient variability.

Brief description of the algorithm used to generate simulation data set is as follows:-

1. Set Boundary Coordinates and limits for STN mass and surrounding region of interest. Arbitrarily fix the location and boundaries for high efficacy spots and outlier spots within that region.

2. Create Normally distributed high and low efficacy data sets.

3. Associate the simulated data set for High/ low efficacy (step 2) with the selected coordinates for Hot, cold and outlier regions (step 1). the selected coordinates were uniformly distributed in the specified area.

4. 3D interpolation of the above data set using interpolation techniques discussed in section 2.4.

5. observation-wise bootstrapping (1000 times) is performed over the above data set. The bootstrapped mean and standard deviation of each voxel in the region were calculated and stored.

45

6. repeat step 2 to 6, for 100 simulations.

7. investigation and evaluation.

In order to evaluate the performance of the statistical optimization, we compared the performance of optimized interpolation with that of direct interpolation in terms of degree of elimination of outliers. The assigned outlier region was checked for number of high efficacy voxels after both direct and optimized interpolation which contributes to their bad score. The improvement due to bootstrapping based optimization is calculated by relative reduction in fake voxels with respective to the number of fake voxels created by direct interpolation.

$$\text{Percentage Improvement} = \left(\frac{G_m - G_d}{G_d} \right) \times 100$$

Where G_d and G_m are the number of voxels assigned in outlier region genuinely representing the real efficacy (and not the fake realization) in direct interpolation and bootstrapping based optimized interpolation respectively.

Additionally, to assess the reliability of the hot spots in the interpolated maps in both the cases, we checked for number of high efficacy voxels that lies within the assigned hot spot region. Here we checked whether the hot spots represented by the interpolation of data lies in real hot region or not. The increment in the percentage reliability of the optimized interpolation method is calculated by

$$\text{Increment in Reliability} = \left(\frac{RD_d - RD_m}{RD_d} \right) \times 100$$

Where, RD_d and RD_m are the relative number of real hot voxel (excluding fake ones) in direct interpolation and bootstrapping based optimized interpolation respectively, calculated as

$$RD = \frac{\text{Real Hot data}(H_r)}{\text{Total Hot data }(H_T)}$$

RESULTS
Bootstrapping based Optimization:

Bootstrapping Result

Figure 3 shows the result of observation-wise bootstrapping. The GUI figures below depicts the interpolation of original data (Linear triangulation method), the mean of the voxelized bootstrapped data and the standard deviation calculated from voxelized bootstrapped data respectively. From the corresponding figures, we can easily notice the reduction in the boundary of interpolated mean plot as compared to that of direct interpolated plot. A high efficacy red spot near location (12,-10) and a low efficacious blue spot near (9, 0) in direct interpolated map are not present in the optimized mean map. The prominent center red (hot) spot persist after bootstrapping based optimization. The third map (right) shows the standard deviation of the bootstrapped interpolated voxels. The values near to zero in case of standard deviation contour maps demonstrate acceptable reliability level of the mean contour.

Simulation Results

(Performance Evaluation for Bootstrapping based Optimization)

The simulation results reveal that the efficacy of bootstrapping improved the immunity of the model from the outliers. The percentage improvement in the outlier handling in bootstrapped interpolated map from direct interpolated map ranges from 0.00% to 59.26% (mean improvement = 6.1922 %). There is a significant improvement in outlier reduction in optimized interpolated model ($t = 4.46$, df = 49, p-value <0.0001). Additionally the increment in the percentage reliability of the optimized interpolation method in representing the real high efficacy data ranges from -56.41% to 80.00% (mean improvement = 12.8775%) as compared to direct interpolation realization. The reliability of high efficacy data is statistically improved after bootstrapping based optimization ($t = 3.63$, df = 49, p-value = 0.0007).
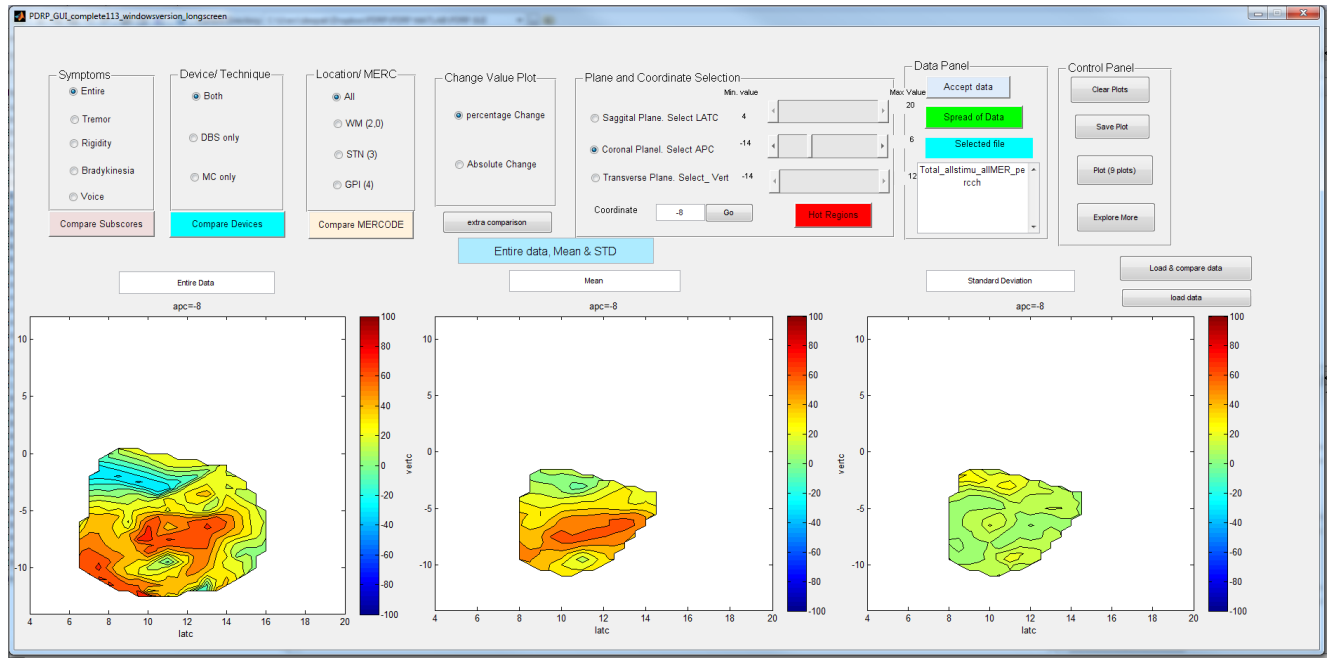
Fig.11. Direct data interpolation (left); Result of bootstrapping: Mean (middle) and standard deviation contours (right)

DISCUSSION

An important step in functional modeling of DBS locations is to enhance the reliability and robustness of the model and to assign the measures of accuracy to the sample estimates by bootstrapping the datasets. Bootstrapping is a computer-based approach to statistical inference based on building a sampling distribution by resampling from the observed data (John Fox). It helps make a rational decision about the population, when uncertainty (introduced by patient and observational variability) is present in our observed data [36]. The main job of bootstrapping optimization procedure is to reduce the effect of outlier data that mislead the realization in case of direct interpolation. In other words, the optimized model should not represent just the observed data but the reliable observed data. The bootstrapping based optimization method employed here provides details on the possible variation of the score level of each voxel in the ROI. The new contour plot produced using the bootstrapped mean values of each voxel are found

48

to be reliably optimized. We're 95% confident that the percentage reliability improvement mean value is included in the interval [5.7%, 20.0%]. Only those data that are supported by significant sample density of similar score level neighbors, are prominently represented in the optimized model. This ensures the score level assigned to each voxel in the optimized model has reduced effect of outlier data. Additionally, for each voxel, the standard deviation of the calculated means score values indicates the spread of the mean of each voxel. This standard deviation is plotted separately which indicates the reliability of the produced mean plot. Hence, simultaneous analysis of the three contour maps, the direct interpolated, bootstrapped mean and bootstrapped standard deviation, provides a better picture of the scenario in terms of locating the most efficacious and reliable regions and also measuring their reliability level. Simulation studies examine the properties of the statistical methods in several scenarios. The stored estimates like mean and variance after each simulation helps check the consistency and identify any outliers or errors. It also enables to explore any trend or pattern if present [37]. Finally, these estimates for all performed simulations, the average estimate over the number of simulations performed is reported as the true estimate of interest (percentage improvement after bootstrapping based optimization = 6.1922 %). We're 95% confident that the percentage outlier improvement mean value is included in the interval [3.4%, 9.0%]. The assessment of the uncertainty in the estimate of interest between simulations is the standard deviation of the estimates from all simulations.

Limitations
factors not considered:

1. Brain size, anatomical differences, patient position. Instrumental errors.

2. Dissimilar location of bony landmarks (calibration or transformation required).

49

INTRODUCTION

Exploring the locations of deep brain to find out optimal spots for electrical stimulation therapy is a challenging task, which need extensive study of DBS efficacy in large number of patients with neuromuscular disorder. In order to find the best location for implanting DBS electrodes, the surgeons explore different electrode tracks during the DBS surgery. The track and the location selected finally for the permanent electrode implantation is based upon the improvement level observed in the patient's PD symptoms during the DBS surgery. Different patients respond distinctly towards stimulation at a particular anatomical location. i.e. The efficacy at these locations varies with every individual patient, specific PD symptom and anatomical location. We already discussed the patient-wise and observational variability in the previous chapters. However, the particular PD symptom at particular location can have different efficacy distribution than the other PD symptoms. It is helpful to analyze efficacy distribution of different symptoms or location at the same time to compare the difference in their high yield regions. Additionally, depending upon the requirements, the user may need to study the yield and reliability of particular region and isolate that region of interest for better understanding. In this chapter, some additional analytical and visualization tools are introduced, which can enhance the understanding and perception of the developed model.

The objective of this study was to develop additional tools that help explore and visualize the STN and surrounding region in the brain for their DBS efficacy. The tools are incorporated into a graphic user interface to facilitate easy usage of all the tools.

METHODS

Production of the Region of Agreement

The aim of this section is to create a confidence region around a high efficacy spot of the

deep brain. A '*mouseclick*' program was developed which on called over a high yield

location in the contour map, highlights the region which follows following conditions:

> (a) the voxel coordinates in vicinity of the selected hot spot (sphere of radius 4 mm
>
> around the selected point);
>
> (b) the locations having percentage efficacy level within the range of $\pm$ 10 the
>
> efficacy level of the selected point; and
>
> (c) with acceptable reliability ($\pm$ 5 standard deviation).

The output is a confidence region with high efficacy score value and acceptable reliability.

Around each region, with higher mean change score values, a confidence interval is created

by adding the standard deviation to the voxel mean value. This confidence region around the

selected voxel, shows the region of agreement, where the effect of DBS therapy is likely to

be efficient.

Realization of the highest and lowest efficacy spots in the 3D

To create the 3D model of the spots that shows extreme efficacy levels, both high and low in the

ROI, two threshold points were set, to differentiate the middle range and the extreme scores. The

selected voxels with in the required range were than produced in a 3D figure.

Comparison of contour realizations to explore variability among different categories of

data

We developed a MATLAB Graphic User Interface (GUI) that help in analyzing and comparing

contour maps of the interpolated data of different categories. The GUI enables to compare the

51

efficacy spots of various PD symptoms (including, Tremor, Bradykinesia, Rigidity) and different

regions (STN, GPi and surrounding white matter). We can also compare output of direct

interpolation realization, resultant of the bootstrapping optimization and their reliability maps

(standard deviation) at the same point. The complete features and user manual for the

comprehensive GUI can be found in the appendix.

GRAPHIC USER INTERFACE

GUI is an program interface that allows user to intuitively interact with the computer resources

and take advantage of graphics to make the data analysis program more user friendly. In this

study, a large processed database, which includes various optimized spatial interpolation

matrices of different data categories, is saved in the computer system. For 2D and 3D

Visualization of DBS efficacy distribution and simultaneous comparison of various maps a full

functional GUI was developed in MATLAB. **PDRP_GUI** is a user friendly toolbox supporting

intutive menu based operation. It enables the user to directly load any of the required .MAT file

from the database for analysis, study the required details and save the plots of interest.

PDRP_GUI is intended to promote PD DBS efficacy model research and devlopement. The

PDRP_GUI for data analysis is totally functional for users with limited or no experience of

programming and MATLAB software.

2.4.3. Three Dimensional Realization of the highest and lowest efficacy voxels in the ROI:
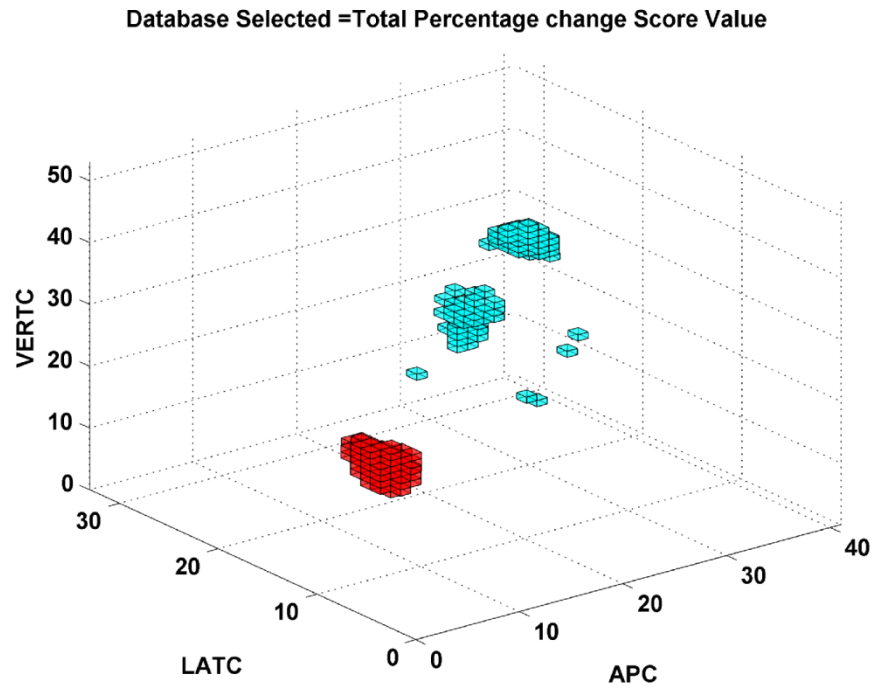

figure.12. Three dimensional realization of high and low yield locations.
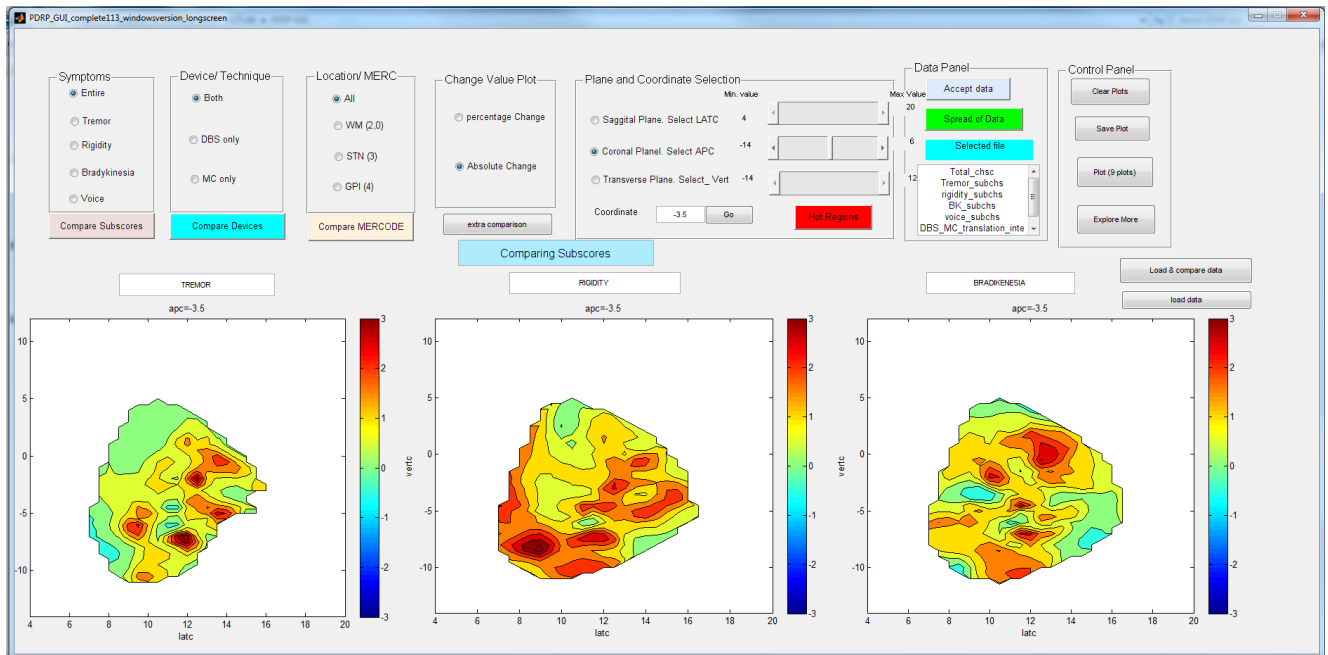
Figure 13. MATLAB GUI comparing Tremor, Rigidity and Bradykinesia a coronal plane.

Figure 13, shows the MATLAB graphic user interface (GUI) developed to help study and compare various contour plots produced from interpolation of different Parkinson disease symptoms, namely Tremor, Rigidity and Bradykinesia. The GUI compares the optimized mean contour of each subscore categories.

CONCLUSION AND FUTURE WORKS
The PDRP_GUI serve the purpose of an interactive tool for analysis and visualization of distribution of DBS efficacy. It shows the particular 3D realization or 2D slices (maps) of the generated model of selected category and configuration. The region of agreement around the efficacious locations indicates the reliable region where DBS electrodes can be implanted for better improvement in PD symptoms. The interpolated contours using MER codes appear to be segregated to different areas as they should. They provide interesting contrasts in areas of efficacy and worsening function. Sub-scores contours display Hot-spots for different PD symptoms separately. Final Vs Rest: We observed that the interpolation of whole data (final with other tracks together) nearly represents a region which comes under the region of agreement of final group. Most of the efficacious area is in the final tracks and most of the negative efficacy is in the other group.

Overlaying : Overlay and data presentation: to fix the plots, the Morel maps and corresponding Contours plots, at correct position and dimensions.

Matching SW atlas / Moral maps with constructed contours.

overlay task and software used Overlay Task: Here our challenge is to fix the plots, the Morel maps and corresponding Contours plots, at correct position (relative to each-other) and dimensions.

54

LIST OF REFERENCES

1.	Jankovic, J., *Parkinson's disease: clinical features and diagnosis.* J Neurol Neurosurg Psychiatry, 2008. **79**(4): p. 368-76.
2.	Samii, A., J.G. Nutt, and B.R. Ransom, *Parkinson's disease.* Lancet, 2004. **363**(9423): p. 1783-93.
3.	Davie, C.A., *A review of Parkinson's disease.* Br Med Bull, 2008. **86**: p. 109-27.
4.	Ben-Shlomo, Y., *How far are we in understanding the cause of Parkinson's disease?* J Neurol Neurosurg Psychiatry, 1996. **61**(1): p. 4-16.
5.	Hughes, A.J., et al., *What features improve the accuracy of clinical diagnosis in Parkinson's disease: a clinicopathologic study. 1992.* Neurology, 2001. **57**(10 Suppl 3): p. S34-8.
6.	Findley, L.J. and L. Cleeves, *The relation of essential tremor to Parkinson's disease.* J Neurol Neurosurg Psychiatry, 1985. **48**(2): p. 192.
7.	Berardelli, A., A.F. Sabra, and M. Hallett, *Physiological mechanisms of rigidity in Parkinson's disease.* J Neurol Neurosurg Psychiatry, 1983. **46**(1): p. 45-53.
8.	Berardelli, A., et al., *Pathophysiology of bradykinesia in Parkinson's disease.* Brain, 2001. **124**(Pt 11): p. 2131-46.
9.	*The Unified Parkinson's Disease Rating Scale (UPDRS): status and recommendations.* Mov Disord, 2003. **18**(7): p. 738-50.
10.	Youdim, M.B. and P. Riederer, *Understanding Parkinson's disease.* Sci Am, 1997. **276**(1): p. 52-9.
11.	Lang, A.E., *When and how should treatment be started in Parkinson disease?* Neurology, 2009. **72**(7 Suppl): p. S39-43.
12.	Deuschl, G., et al., *A randomized trial of deep-brain stimulation for Parkinson's disease.* N Engl J Med, 2006. **355**(9): p. 896-908.
13.	Kikinis, R., et al., *A digital brain atlas for surgical planning, model-driven segmentation, and teaching.* Ieee Transactions on Visualization and Computer Graphics, 1996. **2**(3): p. 232-241.
14.	Lanotte, M.M., et al., *Deep brain stimulation of the subthalamic nucleus: anatomical, neurophysiological, and outcome correlations with the effects of stimulation.* J Neurol Neurosurg Psychiatry, 2002. **72**(1): p. 53-8.
15.	Saint-Cyr, J.A., et al., *Localization of clinically effective stimulating electrodes in the human subthalamic nucleus on magnetic resonance imaging.* J Neurosurg, 2002. **97**(5): p. 1152-66.
16.	Voges, J., et al., *Bilateral high-frequency stimulation in the subthalamic nucleus for the treatment of Parkinson disease: correlation of therapeutic effect with anatomical electrode position.* J Neurosurg, 2002. **96**(2): p. 269-79.

17. Hamel, W., et al., *Subthalamic nucleus stimulation in Parkinson's disease: correlation of active electrode contacts with intraoperative microrecordings.* Stereotact Funct Neurosurg, 2003. **80**(1-4): p. 37-42.

18. Herzog, J., et al., *Most effective stimulation site in subthalamic deep brain stimulation for Parkinson's disease.* Mov Disord, 2004. **19**(9): p. 1050-4.

19. Yokoyama, T., et al., *The optimal stimulation site for chronic stimulation of the subthalamic nucleus in Parkinson's disease.* Stereotact Funct Neurosurg, 2001. **77**(1-4): p. 61-7.

20. Nowinski, W.L., et al., *Statistical analysis of 168 bilateral subthalamic nucleus implantations by means of the probabilistic functional atlas.* Neurosurgery, 2005. **57**(4 Suppl): p. 319-30; discussion 319-30.

21. Nowinski, W.L., et al., *A probabilistic functional atlas of the VIM nucleus constructed from pre-, intra- and postoperative electrophysiological and neuroimaging data acquired during the surgical treatment of Parkinson's disease patients.* Stereotact Funct Neurosurg, 2005. **83**(5-6): p. 190-6.

22. Shenai, M.B., et al., *Construction of relational topographies from the quantitative measurements of functional deep brain stimulation using a 'roving window' interpolation algorithm.* Stereotact Funct Neurosurg, 2010. **88**(1): p. 16-23.

23. Berry, J.K., *Fundamental Operations in Computer-assisted Map Analysis.* International Journal of Geographical Information Systems, 1987. **1**(2): p. 119-136.

24. Zhang, T.C. and W.M. Grill, *Modeling deep brain stimulation: point source approximation versus realistic representation of the electrode.* J Neural Eng, 2010. **7**(6): p. 066009.

25. Lam, *Inverse Distance Weight.* 1983.

26. Bartier, P.M. and C.P. Keller, *Multivariate interpolation to incorporate thematic surface data using inverse distance weighting (IDW).* Computers & Geosciences, 1996. **22**(7): p. 795-799.

27. Bartier, P.M. and C.P. Keller, *Interpolation for geochemical surface reconstruction incorporating topographic catchment definitions.* Mathematical Geology, 1996. **28**(3): p. 253-273.

28. Abdallah, M., et al., *A fuzzy logic model for biogas generation in bioreactor landfills.* Canadian Journal of Civil Engineering, 2009. **36**(4): p. 701-708.

29. Pattin, K.A., et al., *A computationally efficient hypothesis testing method for epistasis analysis using multifactor dimensionality reduction.* Genet Epidemiol, 2009. **33**(1): p. 87-94.

30. QUARTA, C.C.a.F., *Interpolation Methods Comparison.* Computers Math. Applic., 1998. **35**(12): p. 109-126.

31. Sudhyadhom, A., et al., *A high resolution and high contrast MRI for differentiation of subcortical structures for DBS targeting: the Fast Gray Matter Acquisition T1 Inversion Recovery (FGATIR).* Neuroimage, 2009. **47 Suppl 2**: p. T44-52.

32. Ganser, K.A., et al., *A deformable digital brain atlas system according to Talairach and Tournoux.* Med Image Anal, 2004. **8**(1): p. 3-22.

33. Nowinski, W.L., et al., *Multiple brain atlas database and atlas-based neuroimaging system.* Comput Aided Surg, 1997. **2**(1): p. 42-66.

34.   Qu, C.X., et al., *[Study on the development of a choropleth atlas on cancer mortality using the inverse distance weight interpolation in the 1990's].* Zhonghua Liu Xing Bing Xue Za Zhi, 2006. **27**(3): p. 230-3.
35.   Grohmann, C.H. and C. Riccomini, *Comparison of roving-window and search-window techniques for characterising landscape morphometry.* Computers & Geosciences, 2009. **35**(10): p. 2164-2169.
36.   Hesterberg, T., *Control variates and importance sampling for efficient bootstrap simulations.* Statistics and Computing, 1996. **6**(2): p. 147-157.
37.   Burton, A., et al., *The design of simulation studies in medical statistics.* Stat Med, 2006. **25**(24): p. 4279-92.

APPENDIX 1: DBS Intra-operative Rating
Table 6

DBS Intra-operative Rating

Patient: _____ **Side: L / R ► Unilateral ► 1ˢᵗ / 2ⁿᵈ**
Target GPi/STN

Date: _____**Stealth Target Coordinates:** _____ **A/P** _____**Lat** _____**Vert**
_____**Ring** _____**Arc**

Track # _____ **Change from previous:** _____**mm A / P_____ mm M / L**
Microelectrode recording? Y / N

Depth Relative to Target	Stimulator Array				Volts	Tremor			Rigidity			Bradykinesia			Voice	Total	Observations
	0	1	2	3		R	P	Foot	elbow	wrist	leg	Finger Tap	Open/Close	Foot Tap			
Baseline																	

Examiner: _____

APPENDIX 2: GRAPHIC USER INTERFACE (GUI): USER MANUAL

6.1Getting Started

6.2.1 Hardware Requirements: Computer/Workstation: Personal computer with Windows XT,

Vista and Win 7, 2G memory and above is recommended.

6.2.2 Software Requirement: MATLAB, Ver. 7.0 or above, Refer: http://www.mathworks.com/

6.2.3 Download: The database and the program files required for the GUI and analysis are not

yet open to public.

6.1.5 Start up setting

The PDRP_GUI can be set to directly open when MATLAB opens. Create a new m file in the

matlab folder in 'my document' folder. specify the path for the PDRP_GUI.m file

PDRP_GUI;
cd work;

6.1.6 Screen Setting

To set or change the size of GUI figure so that all figure element are easily visible on your

computer screen, following steps should be taken:

1. Debug and Run the PDRP_GUI.m file to check whether the matlab figure is fitting the

   computer screen.

2. Type guide in the MATLAB command screen and select PDRP_GUI.fig.

59
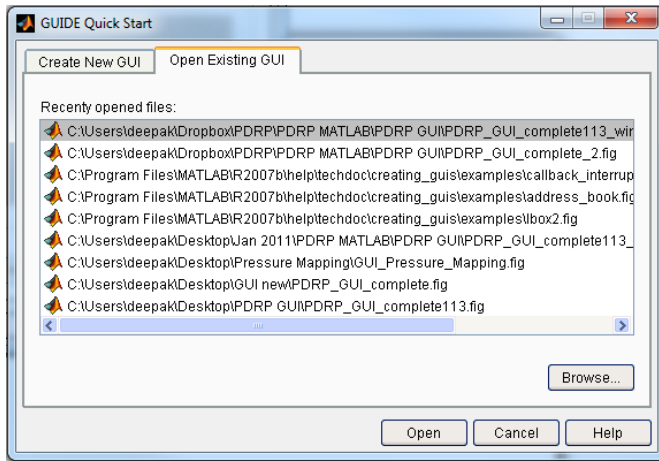
courtesy: MATLAB.7.0

Fig. 15. Guide Quick start window

3. Set the external boundary of the figure to fit it in the screen.

4. set the three axis boundaries and other panels and buttons, if required.

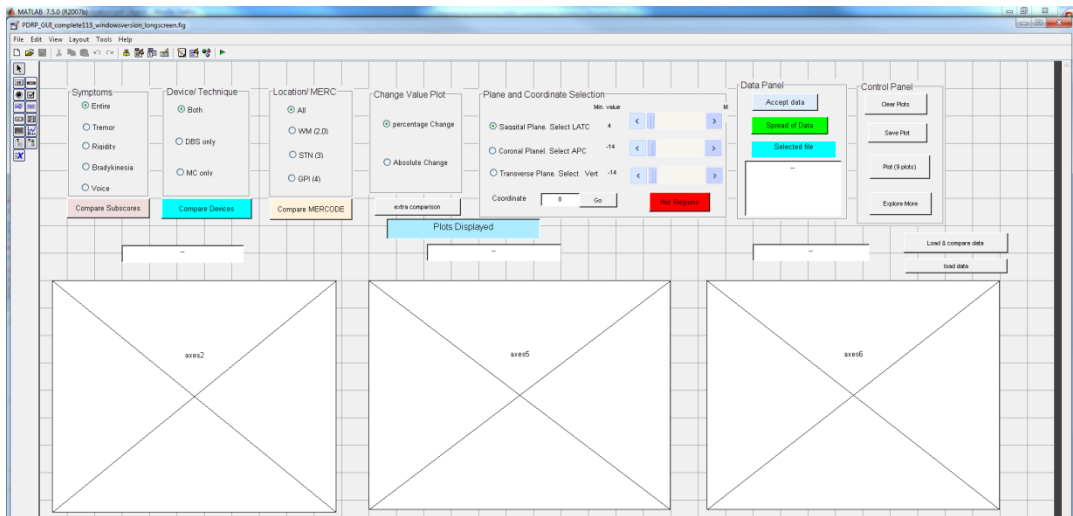5. save your changes and close the .fig file.

fig.

16 snapshot of the matlab figure for screen set.

6.2.4 Debug and Run the PDRP_GUI.m file

6.3 Selection and Loading the Database

60

The software load the database according to the required task intended by the user. The user can select a single category of data set at analyze it direct interpolated model, optimized model and the reliability model simultaneously; or the user can select 3 different categories of dataset to compare their optimized models; or user can manually enter the specific dataset category required for his/her analysis.

6.3.1. Loading Single dataset category:

1. select the required PD symptom (tremor, Bradykinesia, rigidity or voice) for efficacy analysis or select entire data set to study the overall efficacy by clicking the appropriate radio button in the symptom panel (upper left corner).

2. Select the electrode configuration (monopolar DBS, bipolar DBS or both) from technique panel (next to symptom panel).

3. Select the specified location (sub thalamic nucleus, GPi, surrounding white matter or All together).
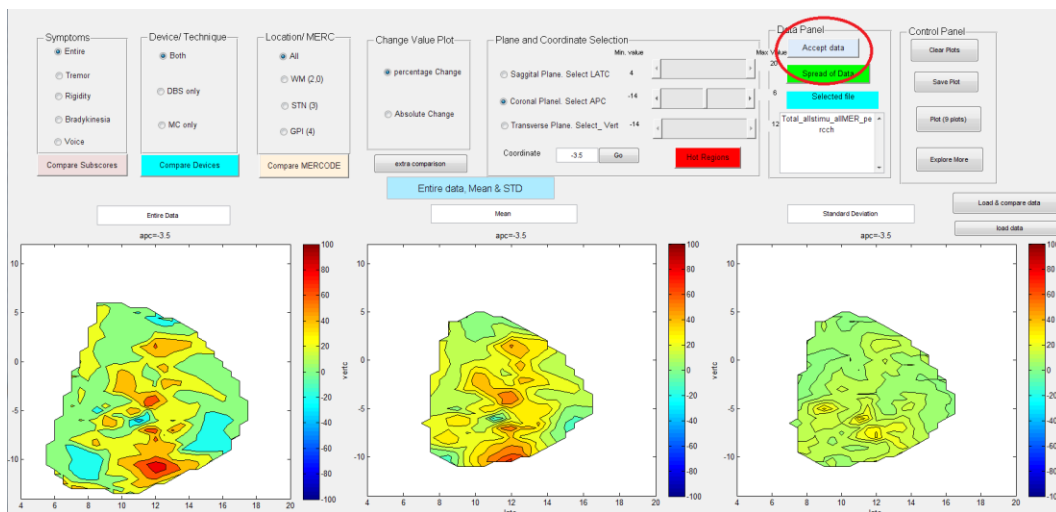
Fig. 17 GUI: selecting, accepting and loading data

4. Select the score value (percentage change score or absolute change score)

5. click the Accept button in data panel to load the selected dataset (fig...).

6. check selected file text box to verify the correct selected file.

6.3.2 Load comparison datasets: (multiple file selection)

1. to compare PD symptom efficacy distribution, follow steps 2-4 of section 6.3.1. click 'compare subscore' button below symptom panel. check selected files text box to verify the correct selected files.

2. to compare electrode configuration efficacy distribution, follow steps 1,3,4 of section 6.3.1. click 'compare technique' button below technique panel. check selected files text box to verify the correct selected files.

3. to compare efficacy distribution at different location, follow steps 1,2, 4 of section 6.3.1. click 'compare locations' button below symptom panel. check selected files text box to verify the correct selected files.
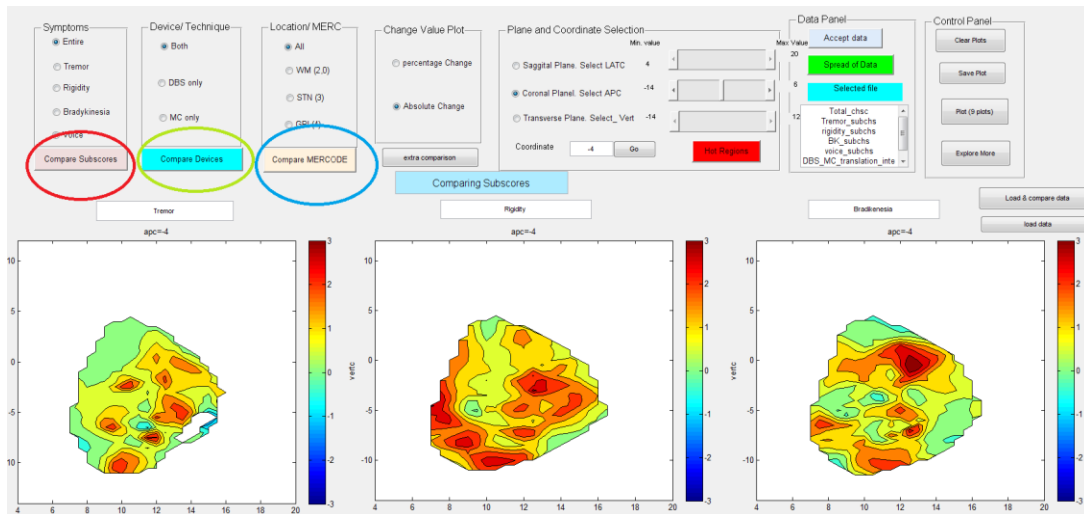
Fig. 18. GUI: Comparison of different data categories.

6.3.3 Load database manually

type the required file name in the 'selected file text box' and click load data button on right of GUI.
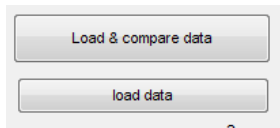

Fig. 19 load new data set.

6.4 Plane and Coordinate Selection

1. Select the intended plane from the three planes, saggital, coronal or transverse plane.

2. select the coordinate by typing intended coordinate in the textbox in plane selection
   panel. and clink 'GO' button.

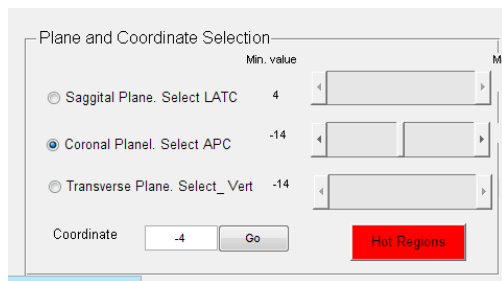3. check the coordinate above each axis's.

Fig. 20 select plane and coordinates.

6.5 Visualization and varying parametrs

1. after loading the database and selecting the appropriate plane and coordinates, click on
   the slider button which is in front of the selected plane.

2. three contour maps will appear in the GUI. The description of the maps can be verified
   from the text box above each axes.

3. at any time the selected plane and coordinates can be varied for differential analysis by
   controlling the three slider buttons. The maximum and minimum limits of the coordinate
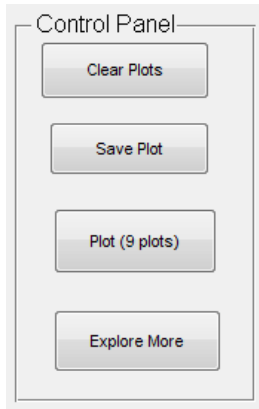   system in the ROI can be check at the ends of sliders.

63

Fig. 21 control panel

6.6 Clear Plots

Clear plots clear the recent plots from the GUI. To visualize the plots we need to reselect the

database category.

6.7 save plots

The GUI can save the recent plot in .bmp; .emf and .fig formats.

6.8 3D visualization

the 'Explore more' button enable the user to study the 3 D realization of the most efficacious
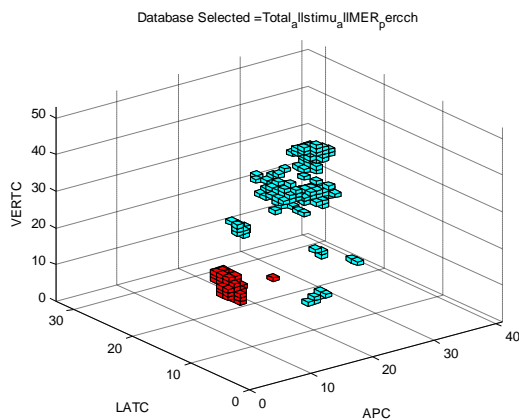

Fig.22 3D visulaization

www.manaraa.com

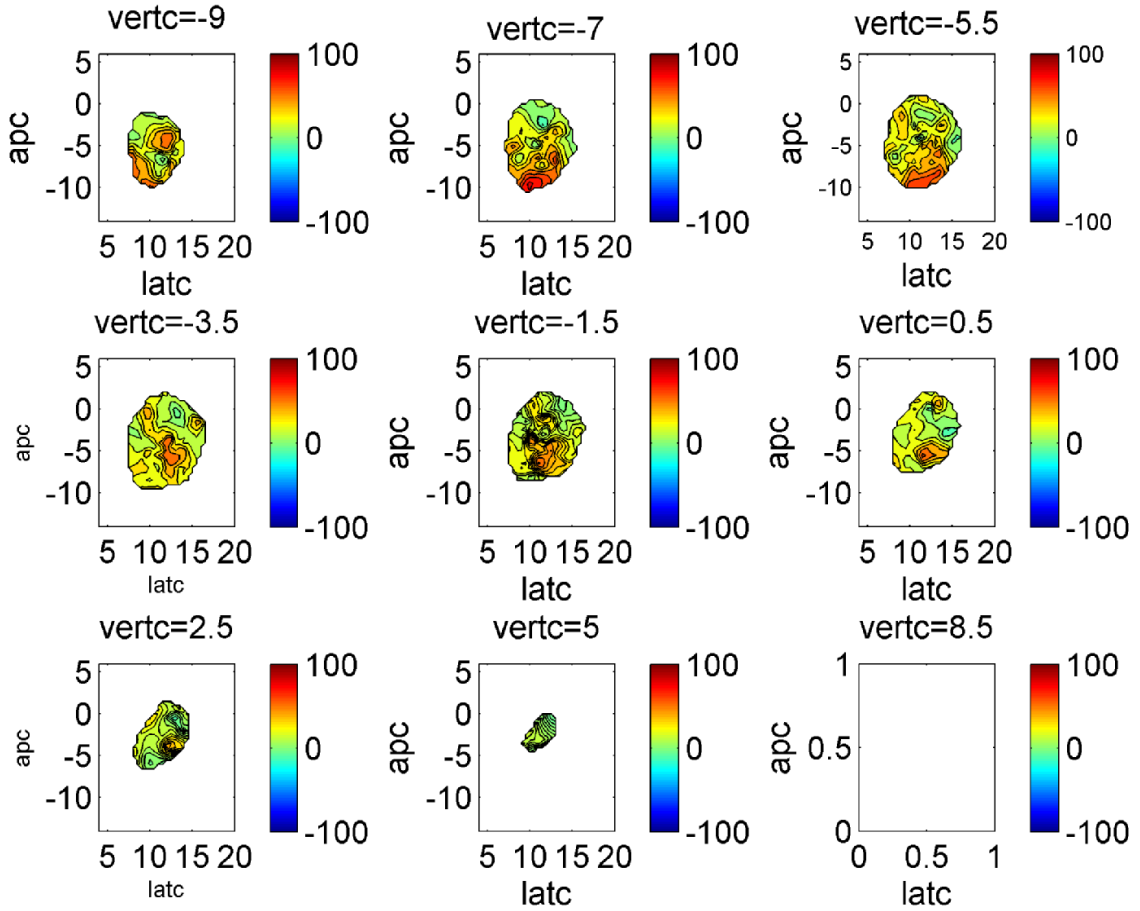## 6.9 Instant Visualization

Fig. 23 instant visualization
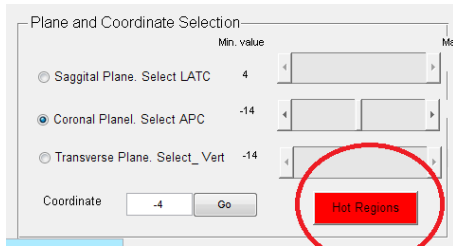
6.10 Hot region

Fig 24. Visualize hot regions

The current version of PDRP_GUI is capable of following task:-

1. select various combinations

change the plane and coordinates to study specific slide,

APPENDIX 3

1D interpolation.

Interpolate a triangle-like signal using an interpolation factor of 5. First, set up signal to be interpolated:

```
y = [0 .5 1 1.5 2 1.5 1 .5 0 -.5 -1 -1.5 -2 -1.5 -1 -.5 0];
N = length(y);
```

Perform the interpolation:

```
L = 5;
M = N*L;
x = 0:L:L*N-1;
xi = 0:M-1;
yi = interpft(y,M);
plot(x,y,'o',xi,yi,'*')
legend('Original data','Interpolated data')
```

66

VITA

Deepak Kumbhare

A. Personal History
    Citizenship: India

B. Educational History

    Virginia Commonwealth University, Richmond, Virginia
    Major: Biomedical Engineering
    Degree: Masters of Science
    Year: 2011
    Thesis: 3D functional modeling of DBS efficacy and Development of analytical tools to
    explore functional STN

    Sri Satya Sai Institute of Science and Technology, R.G.P.V., India
    Major: Biomedical Engineering
    Degree: Bachelor's of Engineering
    Year: 2007

C. Professional Positions
    2007 – Dec 2004
    Life Care Medical Systems Ent. Pvt. Ltd., Mumbai, India
    Service Coordinator and Engineer.